# At Least Nine CMIP6 Climate Models fail the Historical Experiment Test because they do not accurately reproduce the known occurrence of ENSO events and must be withdrawn

Keith Alan Potts[1]

[1]Kyna Keju Pty Ltd

October 9, 2023

**Abstract**

The Historical Experiment (HE) data in the Intergovernmental Panel on Climate Change (IPCC) Climate Model Intercomparison Project six (CMIP6) should demonstrate that all submitted models accurately simulate the climate of the recent past. I show: none of nine models analysed accurately creates the known occurrence of ENSO events; no model agrees with any other; and average aerosol levels of the South East Asian Plume (SEAP), the South AMerican Plume (SAMP) and the West African Plume (WAP) are too low. Additionally, the SEAP and the SAMP cause the global temperature to rise in all nine models and the WAP in six models. Hence these models and all others which cannot accurately portray the known occurrence of ENSO events should be withdrawn from CMIP6 until they can and use of the IPCC Assessment Report six (AR6) should be paused until the effects of these aerosol plumes on the global temperature is re-evaluated.

Posted on 9 Oct 2023 — CC-BY-NC-ND 4 — https://doi.org/10.22541/essoar.169686254.43735786/v1 — This a preprint and has not been peer reviewed. Data may be preliminary.

# At Least Nine CMIP6 Climate Models fail the Historical Experiment Test because they do not accurately reproduce the known occurrence of ENSO events and must be withdrawn

**Keith Alan Potts**[1]

[1] Kyna Keju Pty Ltd.

Corresponding author: Keith Potts (Keith.Potts@bigpond.com)

**Key Points:**

- Nine climate models do not accurately create the known occurrence of ENSO events in the Historical Experiment (HE) in CMIP6
- Additionally, these models do not incorporate aerosols at levels which are consistent with measurements and thus fail the HE test twice
- The IPCC Assessment Report 6 does not recognise that tropical, continental scale, aerosol plumes cause the global temperature to increase

## Abstract

The Historical Experiment (HE) data in the Intergovernmental Panel on Climate Change (IPCC) Climate Model Intercomparison Project six (CMIP6) should demonstrate that all submitted models accurately simulate the climate of the recent past. I show: none of nine models analysed accurately creates the known occurrence of ENSO events; no model agrees with any other; and average aerosol levels of the South East Asian Plume (SEAP), the South AMerican Plume (SAMP) and the West African Plume (WAP) are too low. Additionally, the SEAP and the SAMP cause the global temperature to rise in all nine models and the WAP in six models. Hence these models and all others which cannot accurately portray the known occurrence of ENSO events should be withdrawn from CMIP6 until they can and use of the IPCC Assessment Report six (AR6) should be paused until the effects of these aerosol plumes on the global temperature is re-evaluated.

## Plain Language Summary

The Intergovernmental Panel on Climate Change (IPCC) Assessment Report 6 (AR6) is based on the Climate Model Intercomparison Project six (CMIP6) which required all models to submit the Historical Experiment (HE) data to demonstrate that each model accurately recreates the known climate from 1850 to 2014. This paper demonstrates that nine models from respected institutions fail this test as they do not: reproduce the known sequence of El Nino Southern Oscillation (ENSO) events; nor incorporate aerosol levels consistent with measurements. Additionally, three continental scale, aerosol plumes over south east Asia, West Africa and Amazonia are shown to increase the global temperature by restricting convection in the area of the plume, a fact not recognised by the IPCC. CMIP6 and AR6 should therefore be withdrawn until the climate models are retuned using measured aerosol levels and the effects of these three plumes on the global temperature reassessed after actual aerosol levels are incorporated.


## 1. Introduction

### 1.1. Areas

The areas used in this analysis are shown in the Supporting Information and are: SEAP Area 10º S-10º N and 90º E-160º E; SAMP Area 10º-15º S and 55º-65º W; WAP Area 0º-10º N 0º–10º E and the Nino 3.4 Area 5º S-5º N and 120º-170º W.

### 1.2. IPCC

The IPCC Assessment Report Six (AR6) (Core Writing Team, 2023) is based on CMIP6 which included the HE (Eyring et al., 2016).

### 1.3. Models

Models from the UK Met Office (Ridley et al., 2019), NASA (Studies, 2019), NOAA (Krasting et al., 2018), CESM2 (NCAR) (Danabasoglu, 2019), Canada (Swart et al., 2019), Japan (Shiogama et al., 2019), France (Seferian, 2018), Norway (Seland et al., 2019) and CSIRO (Australia) (Ziehn et al., 2019) are analysed.

### 1.4. ENSO

ENSO events are the greatest variation in the global climate (McPhaden et al., 2006), (Johnson, 2013) and are characterised by a sea surface temperature (SST) 0.5ºC above the long-term average SST in the Nino 3.4 Area in the central Pacific Ocean and have global and regional effects on the climate (UK-Met-Office, 2023) and on the global temperature (Geng et al., 2023; Privalsky & Jensen, 1995; Tsonis et al., 2005).

## 2. Methods

The correct creation of ENSO events in climate models is crucial and the CMIP6 HE is designed to demonstrate that the models do precisely this. First using the above ENSO definition and the SST in the Nino 3.4 Area from the HadISST1 dataset (Rayner et al., 2003), at https://psl.noaa.gov/gcos_wgsp/Timeseries/Nino34/ (1870 – 2014) the HE years are classed as ENSO or non-ENSO years and then compared with the SST in the same area from each of the models. Second the power spectrum of the SST in the Nino 3.4 Area from HadISST1 is compared to the power spectra of the SST in the Nino 3.4 Area from each of the nine models individually.

I also show that:

1. The AOD levels of the SEAP, SAMP and WAP do not match historical measurements in the HE which they should;
2. The SEAP has a statistically significant connection to ENSO whilst the SAMP and WAP do not.
3. The SEAP, SAMP and WAP have strong connections to the global temperature.

## 3. Data and Results

Data is derived from CMIP 6, the Terra satellite (Kaufman et al., 2000) and the NCEP reanalysis (Kalnay et al., 1996).

### 3.1 Aerosols

Aerosols are solid or liquid particles suspended in the atmosphere (Farmer et al., 2021) and are the greatest source of uncertainty in climate modelling (Kahn et al., 2023). Eight continental scale aerosol plumes now exist each year and are described in the Supporting Information. The Aerosol Optical Depth (AOD) of the SEAP Area from the nine models and Terra (2000-2022) is shown in Fig.2(a) with the carbon dioxide ($CO_2$) levels (Meinshausen et al., 2017). It is clear from Fig. 2(a) that the AOD levels in the SEAP Area are significantly underrepresented in the nine models compared with the Terra data. Only the NOAA data is close. Across the nine models only 1.95% (29 of 1,485 months) of the AOD levels fall within the Terra data range when about 20% should be expected to fall in this range from 1980 to 2014. Hence the models are underrepresenting the occurrence of SEAP Area AOD in this period by an order of magnitude and the average AOD from the nine models is only 46% of the average Terra AOD.

All models show similar trajectories for the SEAP Area AOD levels from 1850 to 2014 – steady to 1950 then increasing to 2014 even though the absolute values are significantly different. Fig. 2(b) shows the average SEAP Area AOD and $CO_2$ percentage changes since 1850 which are nearly identical although the SEAP AOD shows much greater variability in recent years which is relevant in the context of the recent global temperature trajectory.

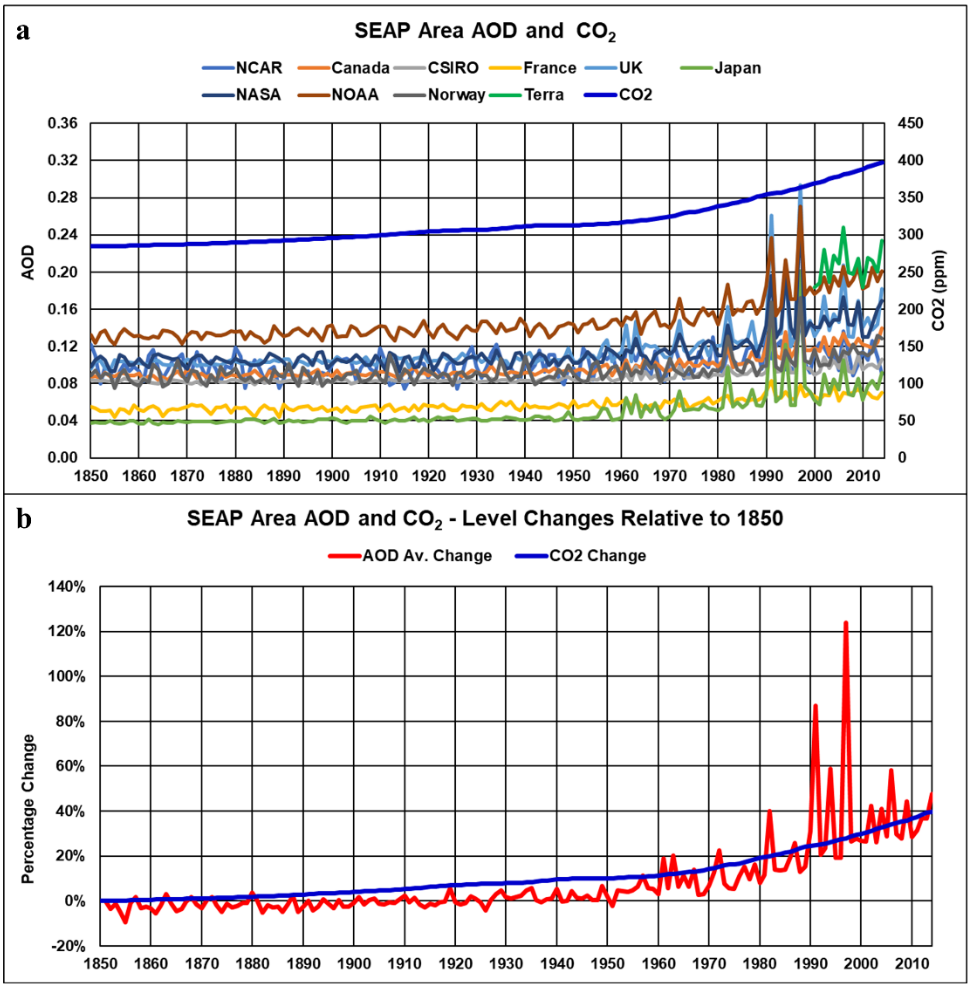


Figure 1: SEAP Area AOD from the nine models and Terra and $CO_2$ (a). percentage changes (b).

### 3.2 ENSO

The Supporting Information lists the ENSO/Non-ENSO years with the correlations of the HE models and HadISST1 data (Table S1) and the cross-correlation matrix (Table S2). No model creates a sequence of ENSO events which correctly matches the historical record and, more surprisingly, no model sequence of ENSO events matches any other model.

The power spectra, using PAST3 (Hammer et al., 2001), of each model Nino 3.4 Area SST from the HE and the HadISST1 Nino 3.4 SST data is shown in Fig.1. No model accurately matches the HadISST1 power spectrum which shows major peaks at 3.5 to 3.8 years and at 5.7 years. Only one model, CSIRO, shows a major peak which coincides with the 5.7 year peak whilst the MIROC6 graph (Fig. 2d) uniquely shows only one major peak which is double the power of the next largest, a clear indicator that the model is oscillating at the frequency of the peak.

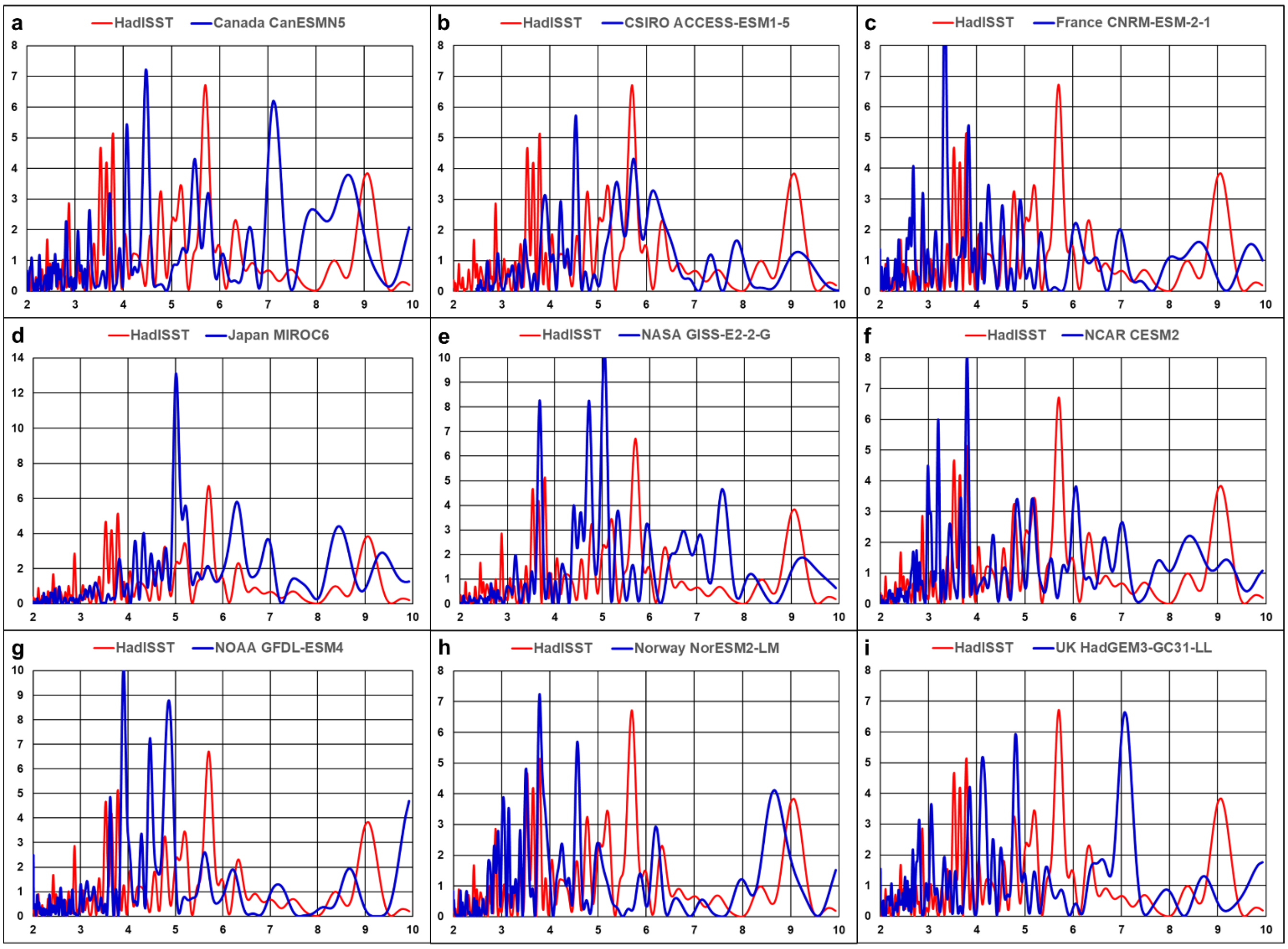


Figure 2: PAST3 Lomb periodogram power spectra (1870-2014) of the Nino 3.4 SST from the HadISST1 dataset and the nine models. The source country/model designation is in the title. The x axis is years and y axis power.

### 3.3. Climate Models and ENSO

Two theories exist to explain the occurrence of ENSO events: (1) a stable mode interacting with High Frequency Forcing (HFF); and (2) a Self-Sustaining Oscillation (SSO) (Wang, 2018) and all climate models are “tuned” and “retuned” to produce, inter alia, the required ENSO return frequency (Hourdin et al., 2017; Mauritsen & Roeckner, 2020; Mignot et al., 2021; Schmidt et al., 2017; Senior et al., 2020). One paper suggests tuning is the most time-consuming process confronted in the development of a climate model, taking up to 3 years. Since the nine models analysed display different occurrences of ENSO events in the HE they must individually incorporate the SSO theory as all the forcing scenarios in the HE are specified (Eyring et al., 2016) and if the HFF theory was being used the models would show at least a modicum of similarity.

Note:

CMIP6 models are assessed for “ENSO Performance” using Planton et al. (2021) and no metric assesses the accurate reproduction of the sequence of known ENSO events in the HE.

The comments re the MIROC6 model oscillation above.

### 3.4. SEAP, SAMP and WAP AOD and ENSO

Fig. 3a, b and c show the SEAP, SAMP and WAP AOD with the SST of the Nino 3.4 Area and Table 1 shows the correlation magnitudes of the AOD of the three plumes and the Nino 3.4 SST.

**SEAP**: It is clear that the SEAP Area AOD levels in the models are much lower than in the Terra measured data. All models show increasing SST in the Nino 3.4 area as the SEAP Area AOD rises. Noting that the AOD levels are too low and that the trend in, for example, the NCAR model is 56ºK/unit AOD. If the average NCAR AOD (0.1) was corrected to the average Terra AOD levels (0.21) along this trend the average Nino 3.4 SST would increase from 300.2ºK to 306.4ºK – an obvious impossibility as the highest Nino 3.4 SST in the NOAA Nino 3.4 long data at https://psl.noaa.gov/gcos_wgsp/Timeseries/Data/nino34.long.data is 301.7ºK. In eight models the statistical significance of the correlation between the SEAP AOD and the Nino 3.4 SST is <0.01 and in one < 0.05. The Terra data shows a very strong correlation much greater than the average of the nine models. Hence in all modelled and measured data there is a statistically strong connection between the SEAP AOD and the Nino 3.4 SST.

**SAMP**: Three models show a positive correlation with the Nino 3.4 SST, four show small positive correlations and two small negative. The average correlation across the nine models is 0.12 which is not significant statistically in the 165-year dataset and the Terra data shows no significant correlation.

**WAP**: Four models show significant positive correlation, three show negative correlations, one statistically significant, and two show no significant correlation. The average is 0.09 which is not significant. The Terra data shows no significant correlation.

Hence the SEAP is unique as it alone shows significantly positive correlations with the Nino 3.4 SST in both the model and Terra data and the Terra data shows correlation magnitudes greater than all but one of the models.

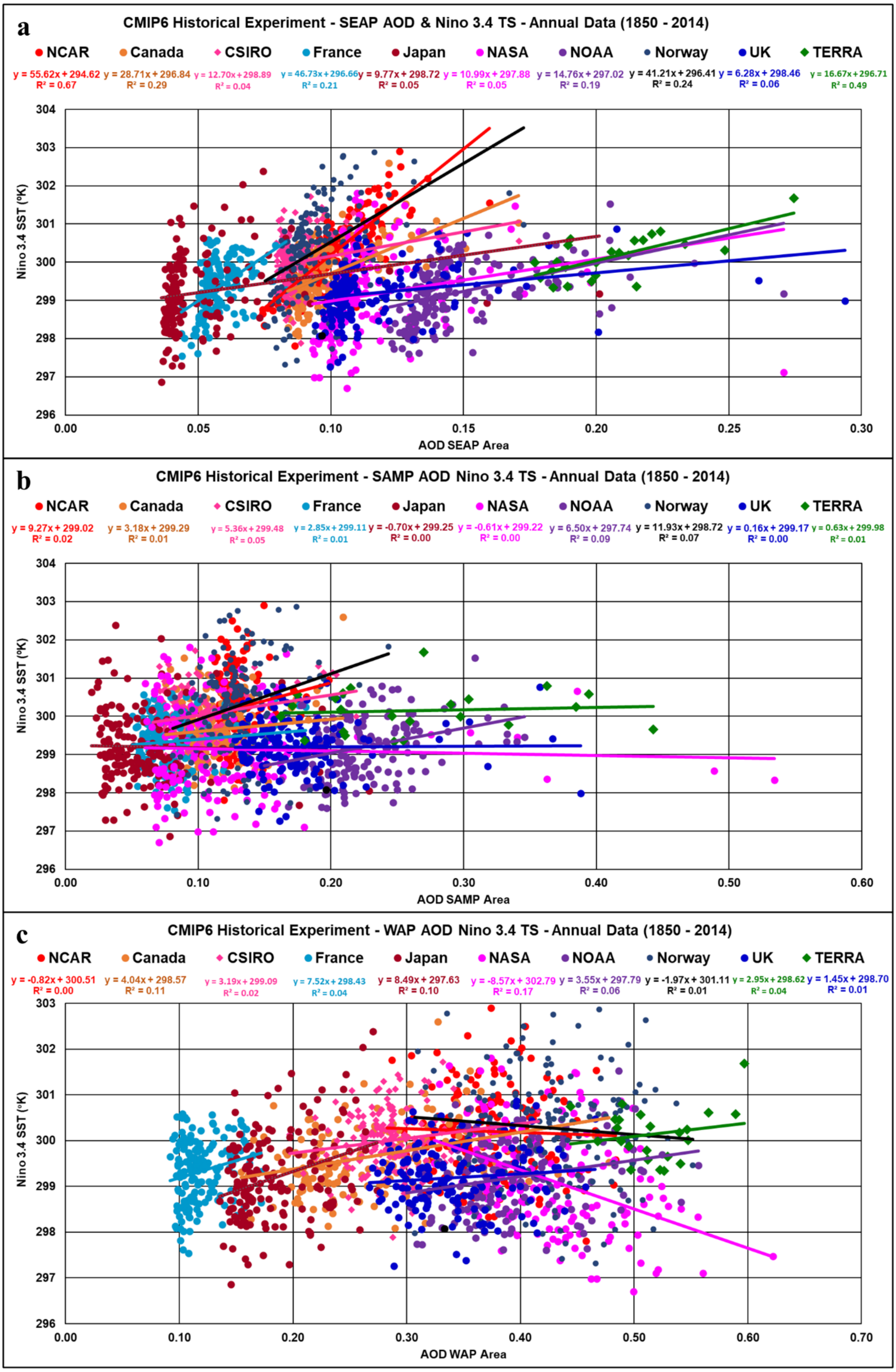
a
CMIP6 Historical Experiment - SEAP AOD & Nino 3.4 TS - Annual Data (1850 - 2014)
NCAR Canada CSIRO France Japan NASA NOAA Norway UK TERRA
y = 55.62x + 294.62 R² = 0.67
y = 28.71x + 296.84 R² = 0.29
y = 12.70x + 298.89 R² = 0.04
y = 46.73x + 296.66 R² = 0.21
y = 9.77x + 298.72 R² = 0.05
y = 10.99x + 297.88 R² = 0.05
y = 14.76x + 297.02 R² = 0.19
y = 41.21x + 296.41 R² = 0.24
y = 6.28x + 298.46 R² = 0.06
y = 16.67x + 296.71 R² = 0.49
Nino 3.4 SST (ºK)
AOD SEAP Area
b
CMIP6 Historical Experiment - SAMP AOD Nino 3.4 TS - Annual Data (1850 - 2014)
NCAR Canada CSIRO France Japan NASA NOAA Norway UK TERRA
y = 9.27x + 299.02 R² = 0.02
y = 3.18x + 299.29 R² = 0.01
y = 5.36x + 299.48 R² = 0.05
y = 2.85x + 299.11 R² = 0.01
y = -0.70x + 299.25 R² = 0.00
y = -0.61x + 299.22 R² = 0.00
y = 6.50x + 297.74 R² = 0.09
y = 11.93x + 298.72 R² = 0.07
y = 0.16x + 299.17 R² = 0.00
y = 0.63x + 299.98 R² = 0.01
Nino 3.4 SST (ºK)
AOD SAMP Area
c
CMIP6 Historical Experiment - WAP AOD Nino 3.4 TS - Annual Data (1850 - 2014)
NCAR Canada CSIRO France Japan NASA NOAA Norway UK TERRA
y = -0.82x + 300.51 R² = 0.00
y = 4.04x + 298.57 R² = 0.11
y = 3.19x + 299.09 R² = 0.02
y = 7.52x + 298.43 R² = 0.04
y = 8.49x + 297.63 R² = 0.10
y = -8.57x + 302.79 R² = 0.17
y = 3.55x + 297.79 R² = 0.06
y = -1.97x + 301.11 R² = 0.01
y = 2.95x + 298.62 R² = 0.04
y = 1.45x + 298.70 R² = 0.01
Nino 3.4 SST (ºK)
AOD WAP Area

Figure 3: SEAP (a), SAMP (b) and WAP (c) AOD and Nino 3.4 SST from the nine models and the Terra satellite.

| | Canada | NCAR | CSIRO | France | UK | Japan | NASA | NOAA | Norway | Average | Terra |
|---|---|---|---|---|---|---|---|---|---|---|---|
| **SEAP** | 0.54 | 0.82 | 0.19 | 0.46 | 0.24 | 0.21 | 0.22 | 0.43 | 0.48 | 0.40 | 0.70 |
| **SAMP** | 0.10 | 0.13 | 0.22 | 0.09 | 0.01 | -0.03 | -0.04 | 0.30 | 0.27 | 0.12 | 0.09 |
| **WAP** | 0.33 | -0.04 | 0.14 | 0.21 | 0.09 | 0.32 | -0.41 | 0.24 | -0.09 | 0.09 | 0.19 |

Table 1 Correlation magnitudes of SEAP, SAMP and WAP AOD and Nino 3.4 SST annual data. Colours show significance: Yellow <0.01, brown <0.02, negative (not significant) light purple negative and significant dark purple.

### 3.5. SEAP, SAMP and WAP AOD and the Annual Global Temperature

Fig. 4a, b and c show the SEAP, SAMP and WAP AOD with the global temperature. All models show the global temperature increasing as the level of aerosols increases in the SEAP Area. The models correlate at an average 0.59 significance <0.01 in all cases and the Terra/NCEP data (2000-2014), with a one-year delay in the temperature data, at 0.52 significance < 0.02. Interestingly all the models except MIROC6 show a much lower global temperature than the NCEP data.

The high correlation between the Terra data and the global temperature the following year is probably because the high levels of SEAP AOD occur late in the year, from September to November (Potts, 2022), which intensifies ENSO events late in the year and with the time the ocean takes to relax from an ENSO event to a neutral state the higher global average temperatures extend into the following year

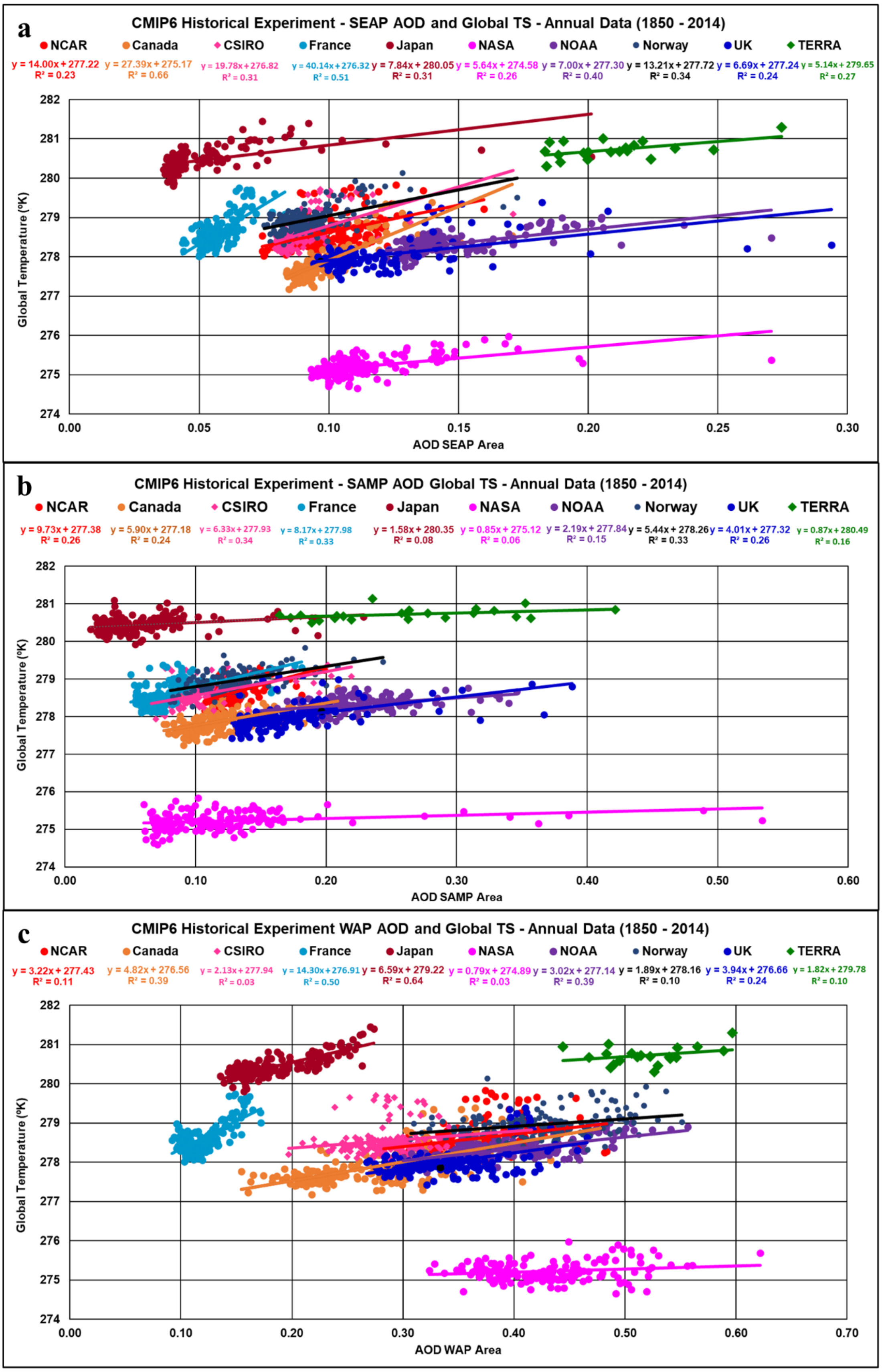


Figure 4: SEAP (a), SAMP (b) and WAP (c) AOD and the global temperature from the nine models and the Terra satellite.

| | Canada | NCAR | CSIRO | France | UK | Japan | NASA | NOAA | Norway | Average | Terra |
|---|---|---|---|---|---|---|---|---|---|---|---|
| **SEAP** | 0.81 | 0.48 | 0.55 | 0.71 | 0.49 | 0.56 | 0.51 | 0.64 | 0.58 | 0.59 | 0.52 |
| **SAMP** | 0.49 | 0.51 | 0.58 | 0.57 | 0.51 | 0.28 | 0.25 | 0.38 | 0.57 | 0.46 | 0.40 |
| **WAP** | 0.62 | 0.33 | 0.17 | 0.70 | 0.49 | 0.80 | 0.17 | 0.63 | 0.31 | 0.47 | 0.52 |

Table 2: Correlation magnitudes SEAP, SAMP and WAP AOD and global temperature for the nine models, the average and Terra data. Colours show significance: Yellow <0.01, brown <0.02, green <0.05, blue <0.10.

### 3.6. Aerosols, Convection and The Global Temperature

Heat can be moved between two points by conduction, convection and radiation. Conduction is impossible in the atmosphere leaving convection and radiation to remove the heat the Earth absorbs daily from the sun. The SEAP Area covers an area 4,842 by 1,383 Km or $6.7*10^{12}$ $m^2$ and convection reduces significantly in times of high AOD. The nine models show average omega at 700 hPa in the SEAP Area at -0.034 Pa/s with an average increase of 0.042 Pa/s per unit increase in AOD which with an AOD average range of 0.12 implies a reduction in convection of 0.005Pa/s or 14% from minimum to maximum AOD. The Last Millennium Ensemble (LME) (Otto-Bliesner et al., 2016), Terra/NCEP and MERRA2 (Gelaro et al., 2017) also show a reduction in convection in the SEAP Area as the SEAP AOD rises (Potts, 2022) and in the WAP Area as the WAP AOD rises in (Potts, 2021). This reduction of convection over such immense areas will result in a significant reduction in the heat removed from the Earth's surface by convection and therefore cause in an increase in the global temperature.

It is also worth noting that removing heat from the Earth's surface by convection in the tropics rather than by radiation negates the effects of most of the greenhouse gases in the atmosphere as convection raises the warm air to the top of the troposphere, about 17 Km altitude (110 hPa pressure), which is then above about 90% of the atmosphere.

### 3.7. Recommendations for Future Work

Future work to develop models which can replicate the known occurrence of ENSO events should incorporate the HFF theory. This theory is outlined in detail in (Potts, 2022) which shows that the SEAP Area hosted over 26% of the global volcanic eruptions (Venzke, 2013) since 1800 and confirms the close association between the AOD in the SEAP Area and the Nino 3.4 SST using the LME, MERRA-2 and Terra/NCEP datasets. This paper also shows: the power spectra of the Nino 3.4 SST (HadlSST_1) and volcanic tephra in Fig. 3 which are much closer in form than any of the nine models analysed here; and outlines the sources of the SEAP Area volcanic and anthropogenic aerosols in the Supporting Information. Therefore, given the failure of the SSO theory of ENSO to create the known sequence of ENSO events in the CMIP6 HE and the close association of the SEAP Area AOD and the Nino 3.4 SST in many datasets it is surely time to use HFF by SEAP Area aerosols combined with emissions which create the known levels of aerosols in the areas of all eight continental scale aerosol plumes. This will automatically create ENSO events at the time of high SEAP Area AOD and will force all nine models to replicate the known sequence of ENSO events as they all show a statistically significant connection between the SEAP Area AOD and the Nino 3.4 SST.

It is also worth noting that the global $CO_2$ levels and the AOD of the SEAP Area show the same percentage increases over the HE period in Fig. 2b and both show a connection to the global temperature. It is therefore crucial to disentangle the individual effects of $CO_2$ and these aerosol plumes on the global temperature to enable mitigation of each to be undertaken.

Therefore, the nine climate models and all others with similar flawed characteristics should be retuned using AOD levels which match the Terra AOD data and not the very low preindustrial AOD levels. This will force the incorporation of the effects of the SEAP, SAMP and WAP on the global temperature into the models and this will undoubtably require a reassessment of the effects of greenhouse gases within the models and the sensitivity of the models to greenhouse gas levels may well have to be reduced, possibly substantially.

## 4. Conclusions

The nine models analysed fail to:

1. Create the known sequence of ENSO events in the CMIP6 HE;
2. Agree on the sequence of ENSO events between themselves;
3. Accurately incorporate the AOD of the SEAP, the SAMP and the WAP in the models; and

the IPCC fails to acknowledge that the SEAP, the SAMP and the WAP force the global temperature higher stating only in AR6 that "Observed warming is driven by emissions from human activities, with greenhouse gas warming partly masked by aerosol cooling".

For these reasons:

1. All the nine climate models are obviously fatally flawed and should be withdrawn from CMIP6;
2. All other models with the same flawed characteristics should also be withdrawn; and
3. Use of the IPCC AR6 should be paused until the effects of the SEAP, SAMP and WAP aerosol plumes on the global temperature are fully understood as we may be only addressing one issue when, in fact, there may be nine (greenhouse gases plus eight plumes) requiring attention and we have no understanding of their relative importance at present!

## Acknowledgments

I acknowledge: NASA: The analyses and visualizations used in this paper were produced with the Giovanni online data system, developed and maintained by the NASA GES DISC and the mission scientists and Principal Investigators who provided the data used in this paper. Google Earth™ and the copyright holders noted for the images of the Earth;

## Conflict Of Interest

The author declares no conflicts of interest relevant to this study

## Open Research

Data and Software Availability Statement

No new data was created in this research project. Original data and software is cited in the references and is available at:

**CMIP6 data**: https://esgf-index1.ceda.ac.uk/search/cmip6-ceda/

**Last Millennium Ensemble data**: https://www.earthsystemgrid.org/

**NASA Terra and MERRA2 data**: https://giovanni.gsfc.nasa.gov/giovanni/

**NCEP Reanalysis data**: https://psl.noaa.gov/cgi-bin/data/timeseries/timeseries1.pl

**Volcanic Eruption data:** https://volcano.si.edu/

**HadISST1 Nino 3.4 SST:** https://psl.noaa.gov/gcos_wgsp/Timeseries/Nino34/

**Greenhouse gas concentrations:** https://www.climatecollege.unimelb.edu.au/cmip6

**NOAA gas flare data:** https://www.ngdc.noaa.gov/eog/viirs/download_global_flare.html

**NOAA Images:** https://psl.noaa.gov/data/gridded/reanalysis/

**Dr Robert Schmunk - Panoply:** https://www.giss.nasa.gov/tools/panoply/ **(netcdf data viewer)**

## References


Core Writing Team, H. L. a. J. R. e. (2023). *IPCC, 2023: Climate Change 2023: Synthesis Report. A Report of the Intergovernmental Panel on Climate Change. Contribution of Working Groups I, II and III to the Sixth Assessment Report of the Intergovernmental Panel on Climate Change* Retrieved from Geneva:

Danabasoglu, G. (2019). NCAR CESM2 model output prepared for CMIP6 CMIP historical. Version 2023. Retrieved from https://doi.org/10.22033/ESGF/CMIP6.7627

Eyring, V., Bony, S., Meehl, G. A., Senior, C. A., Stevens, B., Stouffer, R. J., & Taylor, K. E. (2016). Overview of the Coupled Model Intercomparison Project Phase 6 (CMIP6) experimental design and organization. *Geosci. Model Dev., 9*(5), 1937-1958. https://gmd.copernicus.org/articles/9/1937/2016/

Farmer, D. K., Boedicker, E. K., & DeBolt, H. M. (2021). Dry Deposition of Atmospheric Aerosols: Approaches, Observations, and Mechanisms. *Annual Review of Physical Chemistry, 72*(1), 375-397. https://www.annualreviews.org/doi/abs/10.1146/annurev-physchem-090519-034936

Gelaro, R., McCarty, W., Suárez, M. J., Todling, R., Molod, A., Takacs, L., et al. (2017). The Modern-Era Retrospective Analysis for Research and Applications, Version 2 (MERRA-2). *Journal of Climate, 30*(14), 5419-5454. https://journals.ametsoc.org/doi/abs/10.1175/JCLI-D-16-0758.1

Geng, T., Jia, F., Cai, W., Wu, L., Gan, B., Jing, Z., et al. (2023). Increased occurrences of consecutive La Niña events under global warming. *Nature, 619*(7971), 774-781. https://doi.org/10.1038/s41586-023-06236-9

Hammer, Ø., Harper, D. A. T., & Ryan, P. D. (2001). PAST: Paleontological statistics software package for education and data analysis. . *Palaeontologia Electronica 4(1): 9pp*, 9pp.

Hourdin, F., Mauritsen, T., Gettelman, A., Golaz, J.-C., Balaji, V., Duan, Q., et al. (2017). The Art and Science of Climate Model Tuning. *Bulletin of the American Meteorological Society, 98*(3), 589-602. https://journals.ametsoc.org/view/journals/bams/98/3/bams-d-15-00135.1.xml

Johnson, N. C. (2013). How Many ENSO Flavors Can We Distinguish?*. *Journal of Climate, 26*(13), 4816-4827. Article. http://alumni.library.adelaide.edu.au/login?url=http://search.ebscohost.com/login.aspx?direct=true&db=a2h&AN=88906957&site=ehost-live

Kahn, R. A., Andrews, E., Brock, C. A., Chin, M., Feingold, G., Gettelman, A., et al. (2023). Reducing Aerosol Forcing Uncertainty by Combining Models With Satellite and Within-The-Atmosphere Observations: A Three-Way Street. *Reviews of Geophysics, 61*(2), e2022RG000796. https://agupubs.onlinelibrary.wiley.com/doi/abs/10.1029/2022RG000796

Kalnay, E., Kanamitsu, M., Kistler, R., Collins, W., Deaven, D., Gandin, L., et al. (1996). The NCEP/NCAR 40-Year Reanalysis Project. *Bulletin of the American Meteorological Society, 77*(3), 437-471. http://dx.doi.org/10.1175/1520-0477(1996)077<0437:TNYRP>2.0.CO;2

Kaufman, Y. J., Holben, B. N., Tanré, D., Slutsker, I., Smirnov, A., & Eck, T. F. (2000). Will aerosol measurements from Terra and Aqua Polar Orbiting satellites represent the daily aerosol abundance and properties? *Geophysical Research Letters, 27*(23), 3861-3864. http://dx.doi.org/10.1029/2000GL011968

Krasting, J. P., John, J. G., Blanton, C., McHugh, C., Nikonov, S., Radhakrishnan, A., et al. (2018). NOAA-GFDL GFDL-ESM4 model output prepared for CMIP6 CMIP. Retrieved from https://doi.org/10.22033/ESGF/CMIP6.1407

Mauritsen, T., & Roeckner, E. (2020). Tuning the MPI-ESM1.2 Global Climate Model to Improve the Match With Instrumental Record Warming by Lowering Its Climate Sensitivity. *Journal of Advances in Modeling Earth Systems, 12*(5), e2019MS002037. https://agupubs.onlinelibrary.wiley.com/doi/abs/10.1029/2019MS002037

McPhaden, M. J., Zebiak, S. E., & Glantz, M. H. (2006). ENSO as an Integrating Concept in Earth Science. *Science, 314*(5806), 1740-1745. http://science.sciencemag.org/content/sci/314/5806/1740.full.pdf

Meinshausen, M., Vogel, E., Nauels, A., Lorbacher, K., Meinshausen, N., Etheridge, D. M., et al. (2017). Historical greenhouse gas concentrations for climate modelling (CMIP6). *Geosci. Model Dev., 10*(5), 2057-2116. https://gmd.copernicus.org/articles/10/2057/2017/

Mignot, J., Hourdin, F., Deshayes, J., Boucher, O., Gastineau, G., Musat, I., et al. (2021). The Tuning Strategy of IPSL-CM6A-LR. *Journal of Advances in Modeling Earth Systems, 13*(5), e2020MS002340. https://agupubs.onlinelibrary.wiley.com/doi/abs/10.1029/2020MS002340

Otto-Bliesner, B. L., Brady, E. C., Fasullo, J., Jahn, A., Landrum, L., Stevenson, S., et al. (2016). Climate Variability and Change since 850 CE: An Ensemble Approach with the Community Earth System Model. *Bulletin of the American Meteorological Society, 97*(5), 735-754. http://journals.ametsoc.org/doi/abs/10.1175/BAMS-D-14-00233.1

Planton, Y. Y., Guilyardi, E., Wittenberg, A. T., Lee, J., Gleckler, P. J., Bayr, T., et al. (2021). Evaluating Climate Models with the CLIVAR 2020 ENSO Metrics Package. *Bulletin of the American Meteorological Society, 102*(2), E193-E217. https://journals.ametsoc.org/view/journals/bams/102/2/BAMS-D-19-0337.1.xml

Potts, K. (2021). Biomass Burning and Gas Flares create the extreme West African Aerosol Plume Which Perturbs the Hadley Circulation and thereby Changes Europe's Winter Climate. *Preprints.org*. https://doi.org/10.20944/preprints202108.0554.v3

Potts, K. (2022). How extreme apparitions of the volcanic and anthropogenic south east Asian aerosol plume trigger and sustain: El Niño and Indian Ocean Dipole events; and drought in south eastern Australia. First attribution and mechanism using Global Volcanism Program, Last Millennium Ensemble, MERRA-2 reanalysis and NASA satellite data. *Atmos. Chem. Phys. Discuss., 2022*, 1-45. https://acp.copernicus.org/preprints/acp-2022-362/

Privalsky, V. E., & Jensen, D. T. (1995). Assessment of the influence of ENSO on annual global air temperatures. *Dynamics of Atmospheres and Oceans, 22*(3), 161-178. https://www.sciencedirect.com/science/article/pii/037702659400400Q

Rayner, N. A., Parker, D. E., Horton, E. B., Folland, C. K., Alexander, L. V., Rowell, D. P., et al. (2003). Global analyses of sea surface temperature, sea ice, and night marine air temperature since the late nineteenth century. *Journal of Geophysical Research: Atmospheres, 108*(D14). https://agupubs.onlinelibrary.wiley.com/doi/abs/10.1029/2002JD002670

Ridley, J., Menary, M., Kuhlbrodt, T., Andrews, M., & Andrews, T. (2019). MOHC HadGEM3-GC31-MM model output prepared for CMIP6 CMIP historical. https://doi.org/10.22033/ESGF/CMIP6.6112

Schmidt, G. A., Bader, D., Donner, L. J., Elsaesser, G. S., Golaz, J. C., Hannay, C., et al. (2017). Practice and philosophy of climate model tuning across six US modeling centers. *Geosci. Model Dev.*, *10*(9), 3207-3223. https://gmd.copernicus.org/articles/10/3207/2017/

Seferian, R. (2018). CNRM-CERFACS CNRM-ESM2-1 model output prepared for CMIP6 CMIP. Retrieved from https://doi.org/10.22033/ESGF/CMIP6.1391

Seland, Ø., Bentsen, M., Olivié, D. J. L., Toniazzo, T., Gjermundsen, A., Graff, L. S., et al. (2019). NCC NorESM2-LM model output prepared for CMIP6 CMIP historical. Retrieved from https://doi.org/10.22033/ESGF/CMIP6.8036

Senior, C. A., Jones, C. G., Wood, R. A., Sellar, A., Belcher, S., Klein-Tank, A., et al. (2020). U.K. Community Earth System Modeling for CMIP6. *Journal of Advances in Modeling Earth Systems, 12*(9), e2019MS002004. https://agupubs.onlinelibrary.wiley.com/doi/abs/10.1029/2019MS002004

Shiogama, H., Abe, M., & Tatebe, H. (2019). MIROC MIROC6 model output prepared for CMIP6 ScenarioMIP. Retrieved from https://doi.org/10.22033/ESGF/CMIP6.898

Studies, N. G. I. f. S. (2019). NASA-GISS GISS-E2-2-G model output prepared for CMIP6 CMIP. Retrieved from https://doi.org/10.22033/ESGF/CMIP6.2081

Swart, N. C., Cole, J. N. S., Kharin, V. V., Lazare, M., Scinocca, J. F., Gillett, N. P., et al. (2019). CCCma CanESM5 model output prepared for CMIP6 CMIP historical-cmip5. Retrieved from https://doi.org/10.22033/ESGF/CMIP6.12553

Tsonis, A. A., Elsner, J. B., Hunt, A. G., & Jagger, T. H. (2005). Unfolding the relation between global temperature and ENSO. *Geophysical Research Letters, 32*(9). https://agupubs.onlinelibrary.wiley.com/doi/abs/10.1029/2005GL022875

UK-Met-Office. (2023). What are El Niño and La Niña? . Retrieved from https://www.metoffice.gov.uk/weather/learn-about/weather/oceans/el-nino

Venzke, E. (2013). *Volcanoes of the World. v. 4.9.1 (17 Sep 2020) http://dx.doi.org/10.5479/si.GVP.VOTW4-2013*.

Wang, C. (2018). A review of ENSO theories. *National Science Review, 5*(6), 813-825. https://doi.org/10.1093/nsr/nwy104

Ziehn, T., Chamberlain, M., Lenton, A., Law, R., Bodman, R., Dix, M., et al. (2019). CSIRO ACCESS-ESM1.5 model output prepared for CMIP6 CMIP. Retrieved from https://doi.org/10.22033/ESGF/CMIP6.2288

# At Least Nine CMIP6 Climate Models fail the Historical Experiment Test because they do not accurately reproduce the known occurrence of ENSO events and must be withdrawn

**Keith Alan Potts[1]**

[1] Kyna Keju Pty Ltd.

Corresponding author: Keith Potts (Keith.Potts@bigpond.com)

**Key Points:**

- Nine climate models do not accurately create the known occurrence of ENSO events in the Historical Experiment (HE) in CMIP6
- Additionally, these models do not incorporate aerosols at levels which are consistent with measurements and thus fail the HE test twice
- The IPCC Assessment Report 6 does not recognise that tropical, continental scale, aerosol plumes cause the global temperature to increase

## Abstract

The Historical Experiment (HE) data in the Intergovernmental Panel on Climate Change (IPCC) Climate Model Intercomparison Project six (CMIP6) should demonstrate that all submitted models accurately simulate the climate of the recent past. I show: none of nine models analysed accurately creates the known occurrence of ENSO events; no model agrees with any other; and average aerosol levels of the South East Asian Plume (SEAP), the South AMerican Plume (SAMP) and the West African Plume (WAP) are too low. Additionally, the SEAP and the SAMP cause the global temperature to rise in all nine models and the WAP in six models. Hence these models and all others which cannot accurately portray the known occurrence of ENSO events should be withdrawn from CMIP6 until they can and use of the IPCC Assessment Report six (AR6) should be paused until the effects of these aerosol plumes on the global temperature is re-evaluated.



## Plain Language Summary

The Intergovernmental Panel on Climate Change (IPCC) Assessment Report 6 (AR6) is based on the Climate Model Intercomparison Project six (CMIP6) which required all models to submit the Historical Experiment (HE) data to demonstrate that each model accurately recreates the known climate from 1850 to 2014. This paper demonstrates that nine models from respected institutions fail this test as they do not: reproduce the known sequence of El Nino Southern Oscillation (ENSO) events; nor incorporate aerosol levels consistent with measurements. Additionally, three continental scale, aerosol plumes over south east Asia, West Africa and Amazonia are shown to increase the global temperature by restricting convection in the area of the plume, a fact not recognised by the IPCC. CMIP6 and AR6 should therefore be withdrawn until the climate models are retuned using measured aerosol levels and the effects of these three plumes on the global temperature reassessed after actual aerosol levels are incorporated.


## 1. Introduction

### 1.1. Areas

The areas used in this analysis are shown in the Supporting Information and are: SEAP Area 10º S-10º N and 90º E-160º E; SAMP Area 10º-15º S and 55º-65º W; WAP Area 0º-10º N 0º–10º E and the Nino 3.4 Area 5º S-5º N and 120º-170º W.

### 1.2. IPCC

The IPCC Assessment Report Six (AR6) (Core Writing Team, 2023) is based on CMIP6 which included the HE (Eyring et al., 2016).

### 1.3. Models

Models from the UK Met Office (Ridley et al., 2019), NASA (Studies, 2019), NOAA (Krasting et al., 2018), CESM2 (NCAR) (Danabasoglu, 2019), Canada (Swart et al., 2019), Japan (Shiogama et al., 2019), France (Seferian, 2018), Norway (Seland et al., 2019) and CSIRO (Australia) (Ziehn et al., 2019) are analysed.

### 1.4. ENSO

ENSO events are the greatest variation in the global climate (McPhaden et al., 2006), (Johnson, 2013) and are characterised by a sea surface temperature (SST) 0.5ºC above the long-term average SST in the Nino 3.4 Area in the central Pacific Ocean and have global and regional effects on the climate (UK-Met-Office, 2023) and on the global temperature (Geng et al., 2023; Privalsky & Jensen, 1995; Tsonis et al., 2005).

## 2. Methods

The correct creation of ENSO events in climate models is crucial and the CMIP6 HE is designed to demonstrate that the models do precisely this. First using the above ENSO definition and the SST in the Nino 3.4 Area from the HadISST1 dataset (Rayner et al., 2003), at https://psl.noaa.gov/gcos_wgsp/Timeseries/Nino34/ (1870 – 2014) the HE years are classed as ENSO or non-ENSO years and then compared with the SST in the same area from each of the models. Second the power spectrum of the SST in the Nino 3.4 Area from HadISST1 is compared to the power spectra of the SST in the Nino 3.4 Area from each of the nine models individually.

I also show that:

1. The AOD levels of the SEAP, SAMP and WAP do not match historical measurements in the HE which they should;
2. The SEAP has a statistically significant connection to ENSO whilst the SAMP and WAP do not.
3. The SEAP, SAMP and WAP have strong connections to the global temperature.

## 3. Data and Results

Data is derived from CMIP 6, the Terra satellite (Kaufman et al., 2000) and the NCEP reanalysis (Kalnay et al., 1996).

### 3.1 Aerosols

Aerosols are solid or liquid particles suspended in the atmosphere (Farmer et al., 2021) and are the greatest source of uncertainty in climate modelling (Kahn et al., 2023). Eight continental scale aerosol plumes now exist each year and are described in the Supporting Information. The Aerosol Optical Depth (AOD) of the SEAP Area from the nine models and Terra (2000-2022) is shown in Fig.2(a) with the carbon dioxide ($CO_2$) levels (Meinshausen et al., 2017). It is clear from Fig. 2(a) that the AOD levels in the SEAP Area are significantly underrepresented in the nine models compared with the Terra data. Only the NOAA data is close. Across the nine models only 1.95% (29 of 1,485 months) of the AOD levels fall within the Terra data range when about 20% should be expected to fall in this range from 1980 to 2014. Hence the models are underrepresenting the occurrence of SEAP Area AOD in this period by an order of magnitude and the average AOD from the nine models is only 46% of the average Terra AOD.

All models show similar trajectories for the SEAP Area AOD levels from 1850 to 2014 – steady to 1950 then increasing to 2014 even though the absolute values are significantly different. Fig. 2(b) shows the average SEAP Area AOD and $CO_2$ percentage changes since 1850 which are nearly identical although the SEAP AOD shows much greater variability in recent years which is relevant in the context of the recent global temperature trajectory.

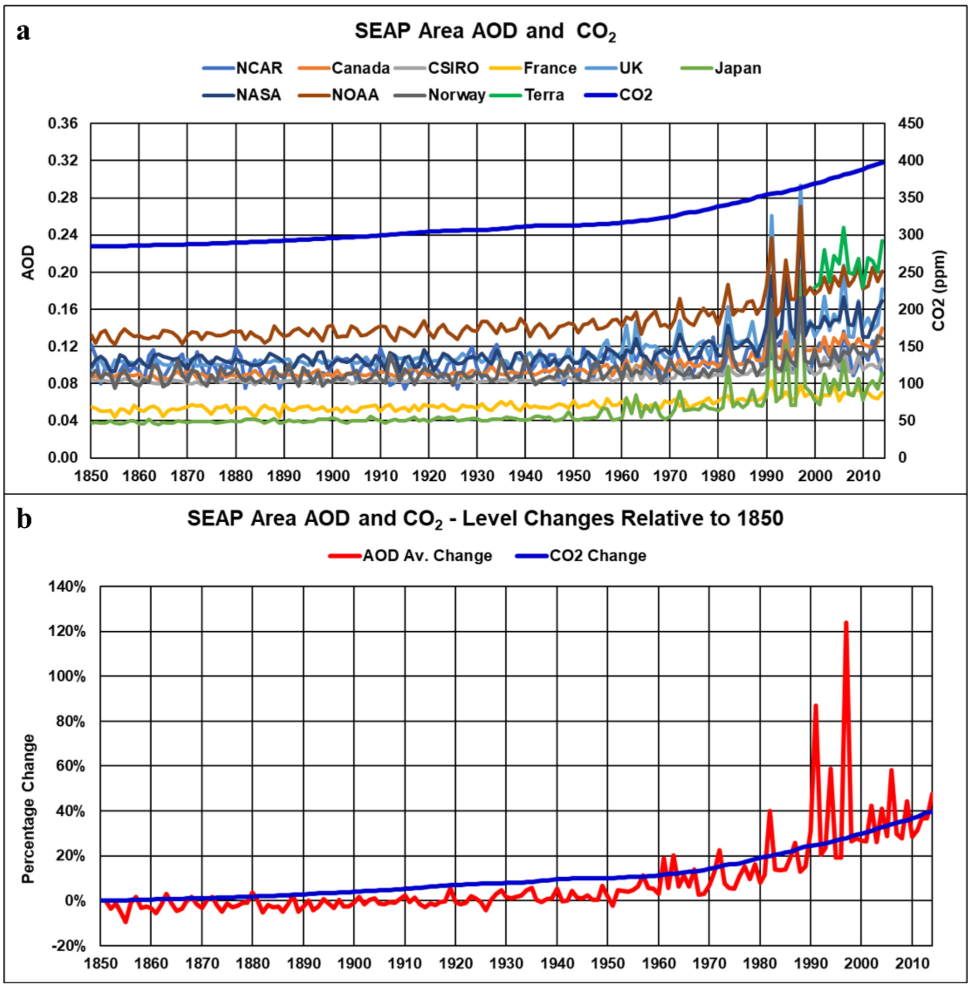


Figure 1: SEAP Area AOD from the nine models and Terra and $CO_2$ (a). percentage changes (b).

### 3.2 ENSO

The Supporting Information lists the ENSO/Non-ENSO years with the correlations of the HE models and HadISST1 data (Table S1) and the cross-correlation matrix (Table S2). No model creates a sequence of ENSO events which correctly matches the historical record and, more surprisingly, no model sequence of ENSO events matches any other model.

The power spectra, using PAST3 (Hammer et al., 2001), of each model Nino 3.4 Area SST from the HE and the HadISST1 Nino 3.4 SST data is shown in Fig.1. No model accurately matches the HadISST1 power spectrum which shows major peaks at 3.5 to 3.8 years and at 5.7 years. Only one model, CSIRO, shows a major peak which coincides with the 5.7 year peak whilst the MIROC6 graph (Fig. 2d) uniquely shows only one major peak which is double the power of the next largest, a clear indicator that the model is oscillating at the frequency of the peak.

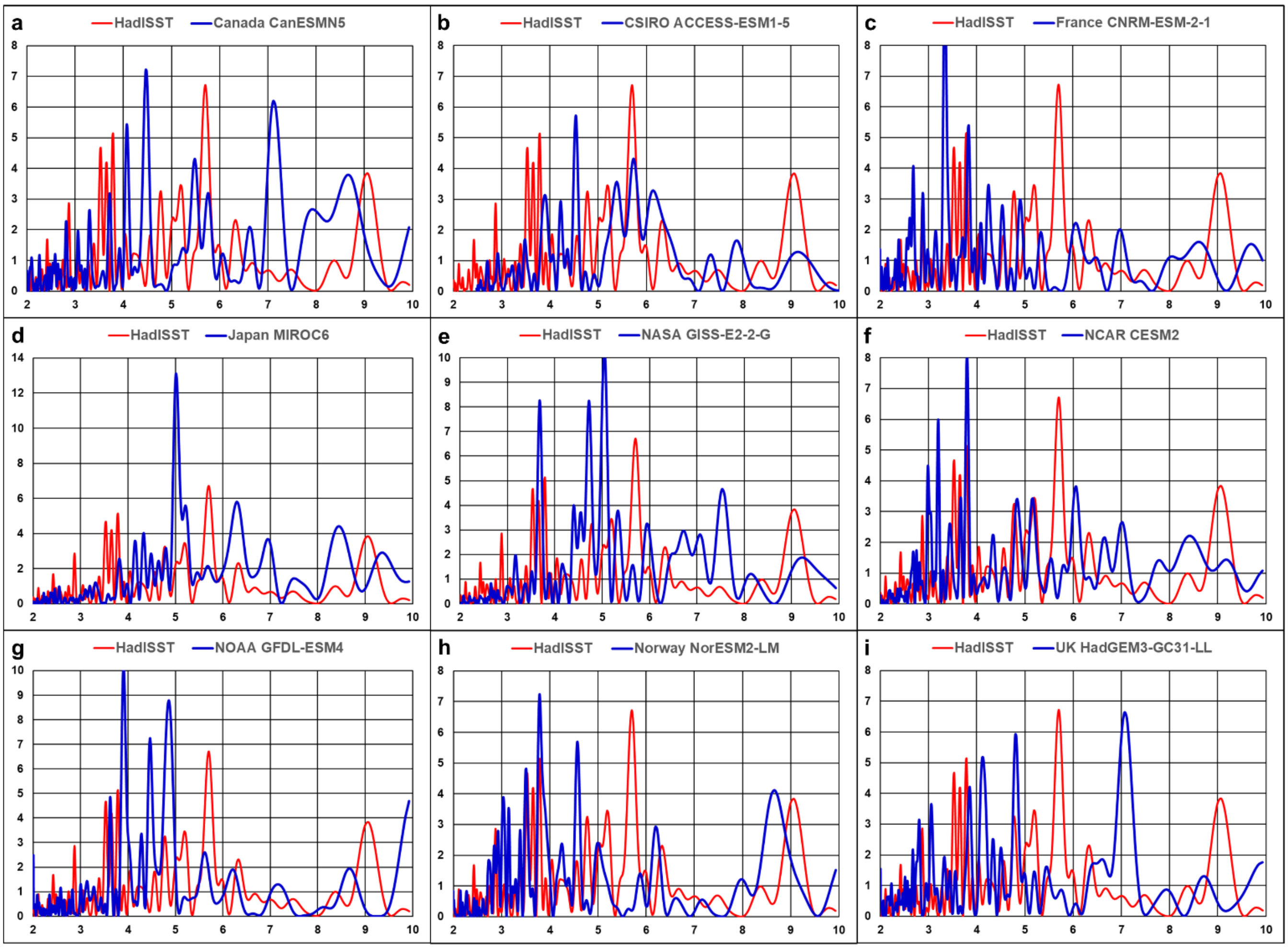


Figure 2: PAST3 Lomb periodogram power spectra (1870-2014) of the Nino 3.4 SST from the HadISST1 dataset and the nine models. The source country/model designation is in the title. The x axis is years and y axis power.

### 3.3. Climate Models and ENSO

Two theories exist to explain the occurrence of ENSO events: (1) a stable mode interacting with High Frequency Forcing (HFF); and (2) a Self-Sustaining Oscillation (SSO) (Wang, 2018) and all climate models are “tuned” and “retuned” to produce, inter alia, the required ENSO return frequency (Hourdin et al., 2017; Mauritsen & Roeckner, 2020; Mignot et al., 2021; Schmidt et al., 2017; Senior et al., 2020). One paper suggests tuning is the most time-consuming process confronted in the development of a climate model, taking up to 3 years. Since the nine models analysed display different occurrences of ENSO events in the HE they must individually incorporate the SSO theory as all the forcing scenarios in the HE are specified (Eyring et al., 2016) and if the HFF theory was being used the models would show at least a modicum of similarity.

Note:

> CMIP6 models are assessed for “ENSO Performance” using Planton et al. (2021) and no metric assesses the accurate reproduction of the sequence of known ENSO events in the HE.
>
> The comments re the MIROC6 model oscillation above.

### 3.4. SEAP, SAMP and WAP AOD and ENSO

Fig. 3a, b and c show the SEAP, SAMP and WAP AOD with the SST of the Nino 3.4 Area and Table 1 shows the correlation magnitudes of the AOD of the three plumes and the Nino 3.4 SST.

**SEAP**: It is clear that the SEAP Area AOD levels in the models are much lower than in the Terra measured data. All models show increasing SST in the Nino 3.4 area as the SEAP Area AOD rises. Noting that the AOD levels are too low and that the trend in, for example, the NCAR model is 56ºK/unit AOD. If the average NCAR AOD (0.1) was corrected to the average Terra AOD levels (0.21) along this trend the average Nino 3.4 SST would increase from 300.2ºK to 306.4ºK – an obvious impossibility as the highest Nino 3.4 SST in the NOAA Nino 3.4 long data at https://psl.noaa.gov/gcos_wgsp/Timeseries/Data/nino34.long.data is 301.7ºK. In eight models the statistical significance of the correlation between the SEAP AOD and the Nino 3.4 SST is $<0.01$ and in one $< 0.05$. The Terra data shows a very strong correlation much greater than the average of the nine models. Hence in all modelled and measured data there is a statistically strong connection between the SEAP AOD and the Nino 3.4 SST.

**SAMP**: Three models show a positive correlation with the Nino 3.4 SST, four show small positive correlations and two small negative. The average correlation across the nine models is 0.12 which is not significant statistically in the 165-year dataset and the Terra data shows no significant correlation.

**WAP**: Four models show significant positive correlation, three show negative correlations, one statistically significant, and two show no significant correlation. The average is 0.09 which is not significant. The Terra data shows no significant correlation.

Hence the SEAP is unique as it alone shows significantly positive correlations with the Nino 3.4 SST in both the model and Terra data and the Terra data shows correlation magnitudes greater than all but one of the models.

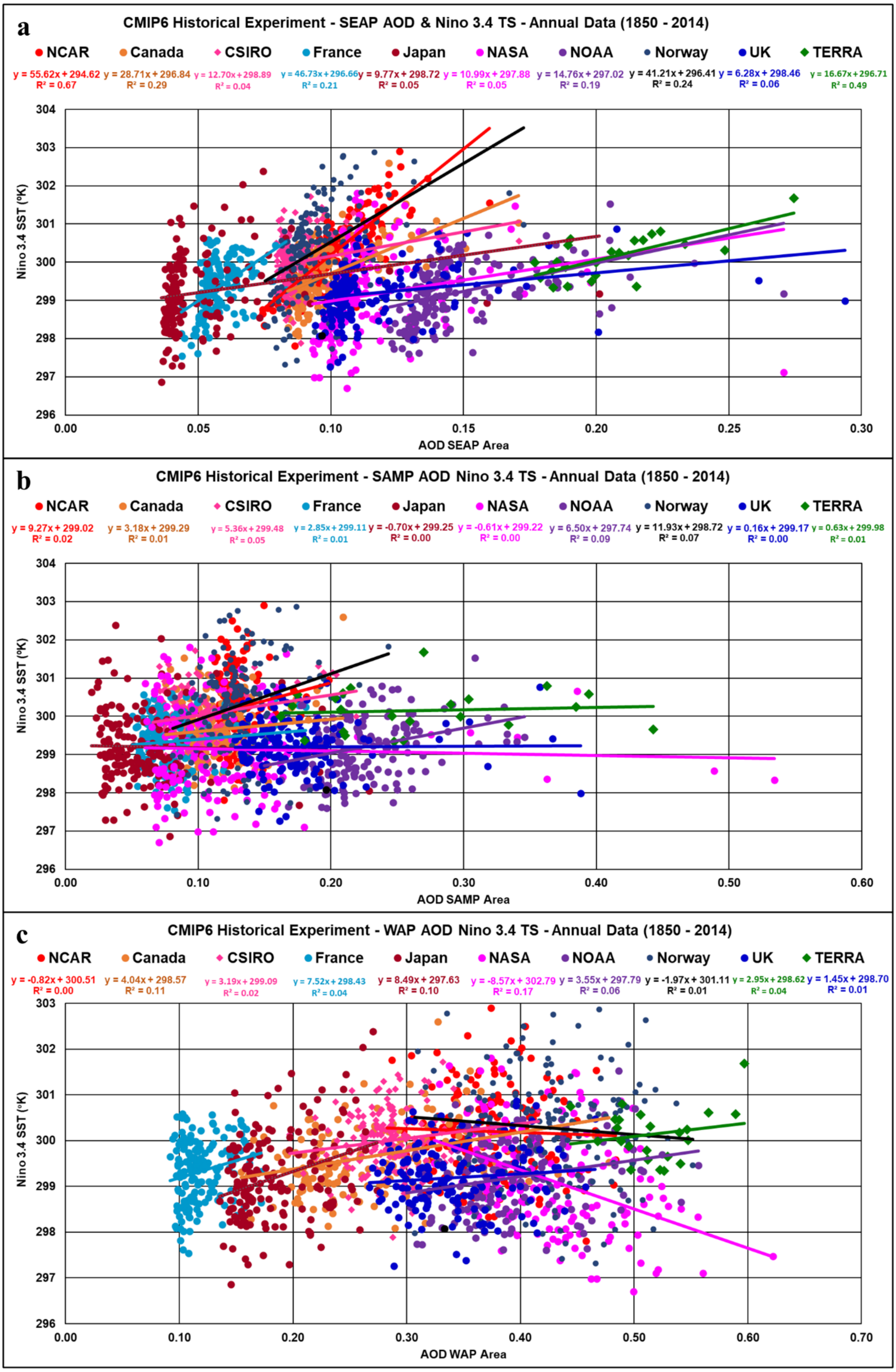
a
CMIP6 Historical Experiment - SEAP AOD & Nino 3.4 TS - Annual Data (1850 - 2014)
NCAR Canada CSIRO France Japan NASA NOAA Norway UK TERRA
y = 55.62x + 294.62 R² = 0.67
y = 28.71x + 296.84 R² = 0.29
y = 12.70x + 298.89 R² = 0.04
y = 46.73x + 296.66 R² = 0.21
y = 9.77x + 298.72 R² = 0.05
y = 10.99x + 297.88 R² = 0.05
y = 14.76x + 297.02 R² = 0.19
y = 41.21x + 296.41 R² = 0.24
y = 6.28x + 298.46 R² = 0.06
y = 16.67x + 296.71 R² = 0.49
Nino 3.4 SST (ºK)
AOD SEAP Area
b
CMIP6 Historical Experiment - SAMP AOD Nino 3.4 TS - Annual Data (1850 - 2014)
NCAR Canada CSIRO France Japan NASA NOAA Norway UK TERRA
y = 9.27x + 299.02 R² = 0.02
y = 3.18x + 299.29 R² = 0.01
y = 5.36x + 299.48 R² = 0.05
y = 2.85x + 299.11 R² = 0.01
y = -0.70x + 299.25 R² = 0.00
y = -0.61x + 299.22 R² = 0.00
y = 6.50x + 297.74 R² = 0.09
y = 11.93x + 298.72 R² = 0.07
y = 0.16x + 299.17 R² = 0.00
y = 0.63x + 299.98 R² = 0.01
Nino 3.4 SST (ºK)
AOD SAMP Area
c
CMIP6 Historical Experiment - WAP AOD Nino 3.4 TS - Annual Data (1850 - 2014)
NCAR Canada CSIRO France Japan NASA NOAA Norway UK TERRA
y = -0.82x + 300.51 R² = 0.00
y = 4.04x + 298.57 R² = 0.11
y = 3.19x + 299.09 R² = 0.02
y = 7.52x + 298.43 R² = 0.04
y = 8.49x + 297.63 R² = 0.10
y = -8.57x + 302.79 R² = 0.17
y = 3.55x + 297.79 R² = 0.06
y = -1.97x + 301.11 R² = 0.01
y = 2.95x + 298.62 R² = 0.04
y = 1.45x + 298.70 R² = 0.01
Nino 3.4 SST (ºK)
AOD WAP Area

Figure 3: SEAP (a), SAMP (b) and WAP (c) AOD and Nino 3.4 SST from the nine models and the Terra satellite.

| | Canada | NCAR | CSIRO | France | UK | Japan | NASA | NOAA | Norway | Average | Terra |
|---|---|---|---|---|---|---|---|---|---|---|---|
| **SEAP** | 0.54 | 0.82 | 0.19 | 0.46 | 0.24 | 0.21 | 0.22 | 0.43 | 0.48 | 0.40 | 0.70 |
| **SAMP** | 0.10 | 0.13 | 0.22 | 0.09 | 0.01 | -0.03 | -0.04 | 0.30 | 0.27 | 0.12 | 0.09 |
| **WAP** | 0.33 | -0.04 | 0.14 | 0.21 | 0.09 | 0.32 | -0.41 | 0.24 | -0.09 | 0.09 | 0.19 |

Table 1 Correlation magnitudes of SEAP, SAMP and WAP AOD and Nino 3.4 SST annual data. Colours show significance: Yellow <0.01, brown <0.02, negative (not significant) light purple negative and significant dark purple.

### 3.5. SEAP, SAMP and WAP AOD and the Annual Global Temperature

Fig. 4a, b and c show the SEAP, SAMP and WAP AOD with the global temperature. All models show the global temperature increasing as the level of aerosols increases in the SEAP Area. The models correlate at an average 0.59 significance <0.01 in all cases and the Terra/NCEP data (2000-2014), with a one-year delay in the temperature data, at 0.52 significance < 0.02. Interestingly all the models except MIROC6 show a much lower global temperature than the NCEP data.

The high correlation between the Terra data and the global temperature the following year is probably because the high levels of SEAP AOD occur late in the year, from September to November (Potts, 2022), which intensifies ENSO events late in the year and with the time the ocean takes to relax from an ENSO event to a neutral state the higher global average temperatures extend into the following year

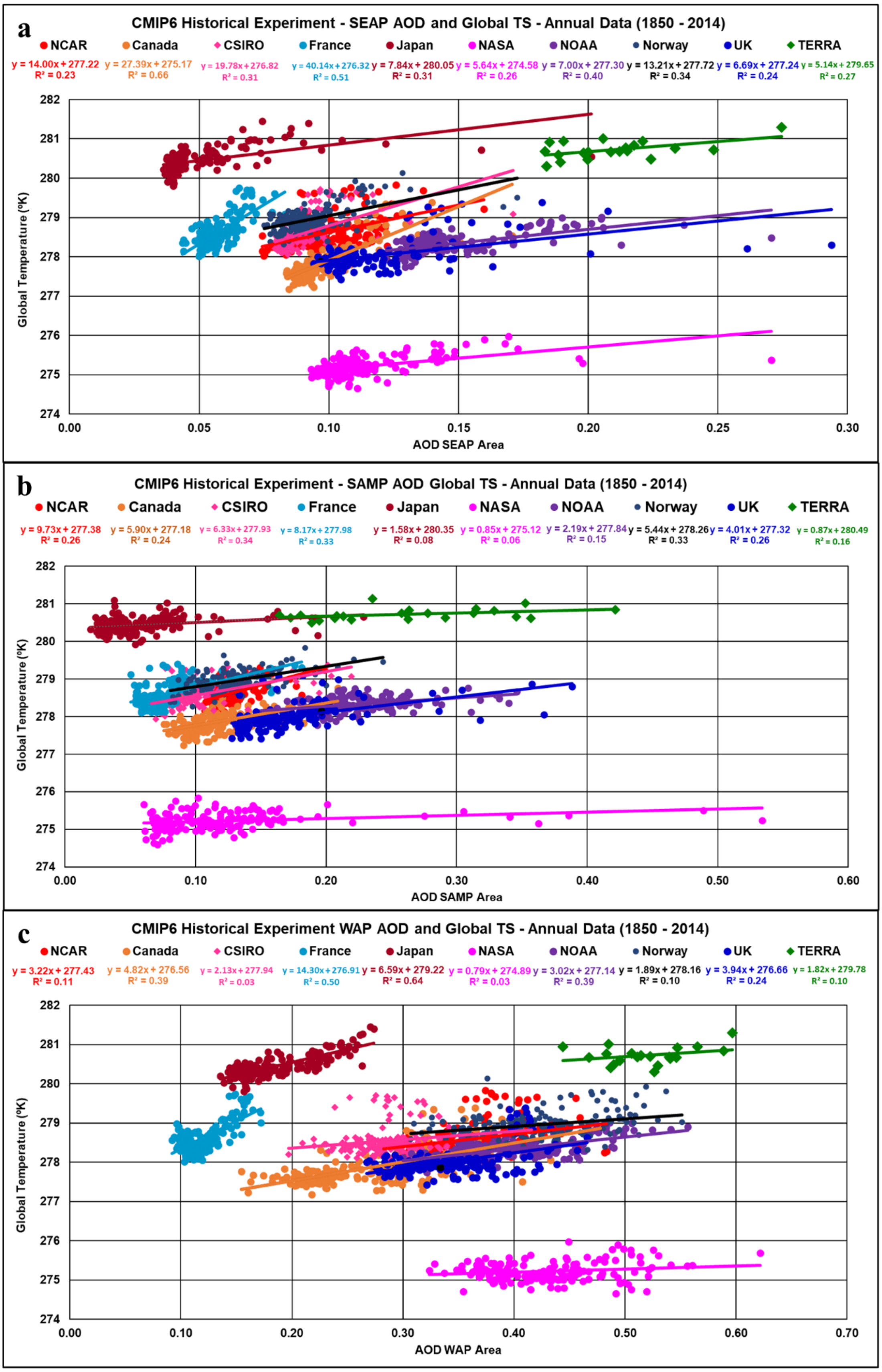


Figure 4: SEAP (a), SAMP (b) and WAP (c) AOD and the global temperature from the nine models and the Terra satellite.

| | Canada | NCAR | CSIRO | France | UK | Japan | NASA | NOAA | Norway | Average | Terra |
|---|---|---|---|---|---|---|---|---|---|---|---|
| **SEAP** | 0.81 | 0.48 | 0.55 | 0.71 | 0.49 | 0.56 | 0.51 | 0.64 | 0.58 | 0.59 | 0.52 |
| **SAMP** | 0.49 | 0.51 | 0.58 | 0.57 | 0.51 | 0.28 | 0.25 | 0.38 | 0.57 | 0.46 | 0.40 |
| **WAP** | 0.62 | 0.33 | 0.17 | 0.70 | 0.49 | 0.80 | 0.17 | 0.63 | 0.31 | 0.47 | 0.52 |

Table 2: Correlation magnitudes SEAP, SAMP and WAP AOD and global temperature for the nine models, the average and Terra data. Colours show significance: Yellow <0.01, brown <0.02, green <0.05, blue <0.10.

### 3.6. Aerosols, Convection and The Global Temperature

Heat can be moved between two points by conduction, convection and radiation. Conduction is impossible in the atmosphere leaving convection and radiation to remove the heat the Earth absorbs daily from the sun. The SEAP Area covers an area 4,842 by 1,383 Km or $6.7*10^{12}$ $m^2$ and convection reduces significantly in times of high AOD. The nine models show average omega at 700 hPa in the SEAP Area at -0.034 Pa/s with an average increase of 0.042 Pa/s per unit increase in AOD which with an AOD average range of 0.12 implies a reduction in convection of 0.005Pa/s or 14% from minimum to maximum AOD. The Last Millennium Ensemble (LME) (Otto-Bliesner et al., 2016), Terra/NCEP and MERRA2 (Gelaro et al., 2017) also show a reduction in convection in the SEAP Area as the SEAP AOD rises (Potts, 2022) and in the WAP Area as the WAP AOD rises in (Potts, 2021). This reduction of convection over such immense areas will result in a significant reduction in the heat removed from the Earth's surface by convection and therefore cause in an increase in the global temperature.

It is also worth noting that removing heat from the Earth's surface by convection in the tropics rather than by radiation negates the effects of most of the greenhouse gases in the atmosphere as convection raises the warm air to the top of the troposphere, about 17 Km altitude (110 hPa pressure), which is then above about 90% of the atmosphere.

### 3.7. Recommendations for Future Work

Future work to develop models which can replicate the known occurrence of ENSO events should incorporate the HFF theory. This theory is outlined in detail in (Potts, 2022) which shows that the SEAP Area hosted over 26% of the global volcanic eruptions (Venzke, 2013) since 1800 and confirms the close association between the AOD in the SEAP Area and the Nino 3.4 SST using the LME, MERRA-2 and Terra/NCEP datasets. This paper also shows: the power spectra of the Nino 3.4 SST (HadlSST_1) and volcanic tephra in Fig. 3 which are much closer in form than any of the nine models analysed here; and outlines the sources of the SEAP Area volcanic and anthropogenic aerosols in the Supporting Information. Therefore, given the failure of the SSO theory of ENSO to create the known sequence of ENSO events in the CMIP6 HE and the close association of the SEAP Area AOD and the Nino 3.4 SST in many datasets it is surely time to use HFF by SEAP Area aerosols combined with emissions which create the known levels of aerosols in the areas of all eight continental scale aerosol plumes. This will automatically create ENSO events at the time of high SEAP Area AOD and will force all nine models to replicate the known sequence of ENSO events as they all show a statistically significant connection between the SEAP Area AOD and the Nino 3.4 SST.

It is also worth noting that the global $CO_2$ levels and the AOD of the SEAP Area show the same percentage increases over the HE period in Fig. 2b and both show a connection to the global temperature. It is therefore crucial to disentangle the individual effects of $CO_2$ and these aerosol plumes on the global temperature to enable mitigation of each to be undertaken.

Therefore, the nine climate models and all others with similar flawed characteristics should be retuned using AOD levels which match the Terra AOD data and not the very low preindustrial AOD levels. This will force the incorporation of the effects of the SEAP, SAMP and WAP on the global temperature into the models and this will undoubtably require a reassessment of the effects of greenhouse gases within the models and the sensitivity of the models to greenhouse gas levels may well have to be reduced, possibly substantially.

## 4. Conclusions

The nine models analysed fail to:

1. Create the known sequence of ENSO events in the CMIP6 HE;
2. Agree on the sequence of ENSO events between themselves;
3. Accurately incorporate the AOD of the SEAP, the SAMP and the WAP in the models; and

the IPCC fails to acknowledge that the SEAP, the SAMP and the WAP force the global temperature higher stating only in AR6 that "Observed warming is driven by emissions from human activities, with greenhouse gas warming partly masked by aerosol cooling".

For these reasons:

1. All the nine climate models are obviously fatally flawed and should be withdrawn from CMIP6;
2. All other models with the same flawed characteristics should also be withdrawn; and
3. Use of the IPCC AR6 should be paused until the effects of the SEAP, SAMP and WAP aerosol plumes on the global temperature are fully understood as we may be only addressing one issue when, in fact, there may be nine (greenhouse gases plus eight plumes) requiring attention and we have no understanding of their relative importance at present!

## Acknowledgments

I acknowledge: NASA: The analyses and visualizations used in this paper were produced with the Giovanni online data system, developed and maintained by the NASA GES DISC and the mission scientists and Principal Investigators who provided the data used in this paper. Google Earth™ and the copyright holders noted for the images of the Earth;

## Conflict Of Interest

The author declares no conflicts of interest relevant to this study

## Open Research

Data and Software Availability Statement

No new data was created in this research project. Original data and software is cited in the references and is available at:

**CMIP6 data**: https://esgf-index1.ceda.ac.uk/search/cmip6-ceda/

**Last Millennium Ensemble data**: https://www.earthsystemgrid.org/

**NASA Terra and MERRA2 data**: https://giovanni.gsfc.nasa.gov/giovanni/

**NCEP Reanalysis data**: https://psl.noaa.gov/cgi-bin/data/timeseries/timeseries1.pl

**Volcanic Eruption data:** https://volcano.si.edu/

**HadISST1 Nino 3.4 SST:** https://psl.noaa.gov/gcos_wgsp/Timeseries/Nino34/

**Greenhouse gas concentrations:** https://www.climatecollege.unimelb.edu.au/cmip6

**NOAA gas flare data:** https://www.ngdc.noaa.gov/eog/viirs/download_global_flare.html

**NOAA Images:** https://psl.noaa.gov/data/gridded/reanalysis/

**Dr Robert Schmunk - Panoply:** https://www.giss.nasa.gov/tools/panoply/ **(netcdf data viewer)**

## References

Core Writing Team, H. L. a. J. R. e. (2023). *IPCC, 2023: Climate Change 2023: Synthesis Report. A Report of the Intergovernmental Panel on Climate Change. Contribution of Working Groups I, II and III to the Sixth Assessment Report of the Intergovernmental Panel on Climate Change* Retrieved from Geneva:

Danabasoglu, G. (2019). NCAR CESM2 model output prepared for CMIP6 CMIP historical. Version 2023. Retrieved from https://doi.org/10.22033/ESGF/CMIP6.7627

Eyring, V., Bony, S., Meehl, G. A., Senior, C. A., Stevens, B., Stouffer, R. J., & Taylor, K. E. (2016). Overview of the Coupled Model Intercomparison Project Phase 6 (CMIP6) experimental design and organization. *Geosci. Model Dev., 9*(5), 1937-1958. https://gmd.copernicus.org/articles/9/1937/2016/

Farmer, D. K., Boedicker, E. K., & DeBolt, H. M. (2021). Dry Deposition of Atmospheric Aerosols: Approaches, Observations, and Mechanisms. *Annual Review of Physical Chemistry, 72*(1), 375-397. https://www.annualreviews.org/doi/abs/10.1146/annurev-physchem-090519-034936

Gelaro, R., McCarty, W., Suárez, M. J., Todling, R., Molod, A., Takacs, L., et al. (2017). The Modern-Era Retrospective Analysis for Research and Applications, Version 2 (MERRA-2). *Journal of Climate, 30*(14), 5419-5454. https://journals.ametsoc.org/doi/abs/10.1175/JCLI-D-16-0758.1

Geng, T., Jia, F., Cai, W., Wu, L., Gan, B., Jing, Z., et al. (2023). Increased occurrences of consecutive La Niña events under global warming. *Nature, 619*(7971), 774-781. https://doi.org/10.1038/s41586-023-06236-9

Hammer, Ø., Harper, D. A. T., & Ryan, P. D. (2001). PAST: Paleontological statistics software package for education and data analysis. . *Palaeontologia Electronica 4(1): 9pp*, 9pp.

Hourdin, F., Mauritsen, T., Gettelman, A., Golaz, J.-C., Balaji, V., Duan, Q., et al. (2017). The Art and Science of Climate Model Tuning. *Bulletin of the American Meteorological Society, 98*(3), 589-602. https://journals.ametsoc.org/view/journals/bams/98/3/bams-d-15-00135.1.xml

Johnson, N. C. (2013). How Many ENSO Flavors Can We Distinguish?*. *Journal of Climate, 26*(13), 4816-4827. Article. http://alumni.library.adelaide.edu.au/login?url=http://search.ebscohost.com/login.aspx?direct=true&db=a2h&AN=88906957&site=ehost-live

Kahn, R. A., Andrews, E., Brock, C. A., Chin, M., Feingold, G., Gettelman, A., et al. (2023). Reducing Aerosol Forcing Uncertainty by Combining Models With Satellite and Within-The-Atmosphere Observations: A Three-Way Street. *Reviews of Geophysics, 61*(2), e2022RG000796. https://agupubs.onlinelibrary.wiley.com/doi/abs/10.1029/2022RG000796

Kalnay, E., Kanamitsu, M., Kistler, R., Collins, W., Deaven, D., Gandin, L., et al. (1996). The NCEP/NCAR 40-Year Reanalysis Project. *Bulletin of the American Meteorological Society, 77*(3), 437-471. http://dx.doi.org/10.1175/1520-0477(1996)077<0437:TNYRP>2.0.CO;2

Kaufman, Y. J., Holben, B. N., Tanré, D., Slutsker, I., Smirnov, A., & Eck, T. F. (2000). Will aerosol measurements from Terra and Aqua Polar Orbiting satellites represent the daily aerosol abundance and properties? *Geophysical Research Letters, 27*(23), 3861-3864. http://dx.doi.org/10.1029/2000GL011968

Krasting, J. P., John, J. G., Blanton, C., McHugh, C., Nikonov, S., Radhakrishnan, A., et al. (2018). NOAA-GFDL GFDL-ESM4 model output prepared for CMIP6 CMIP. Retrieved from https://doi.org/10.22033/ESGF/CMIP6.1407

Mauritsen, T., & Roeckner, E. (2020). Tuning the MPI-ESM1.2 Global Climate Model to Improve the Match With Instrumental Record Warming by Lowering Its Climate Sensitivity. *Journal of Advances in Modeling Earth Systems, 12*(5), e2019MS002037. https://agupubs.onlinelibrary.wiley.com/doi/abs/10.1029/2019MS002037

McPhaden, M. J., Zebiak, S. E., & Glantz, M. H. (2006). ENSO as an Integrating Concept in Earth Science. *Science, 314*(5806), 1740-1745. http://science.sciencemag.org/content/sci/314/5806/1740.full.pdf

Meinshausen, M., Vogel, E., Nauels, A., Lorbacher, K., Meinshausen, N., Etheridge, D. M., et al. (2017). Historical greenhouse gas concentrations for climate modelling (CMIP6). *Geosci. Model Dev., 10*(5), 2057-2116. https://gmd.copernicus.org/articles/10/2057/2017/

Mignot, J., Hourdin, F., Deshayes, J., Boucher, O., Gastineau, G., Musat, I., et al. (2021). The Tuning Strategy of IPSL-CM6A-LR. *Journal of Advances in Modeling Earth Systems, 13*(5), e2020MS002340. https://agupubs.onlinelibrary.wiley.com/doi/abs/10.1029/2020MS002340

Otto-Bliesner, B. L., Brady, E. C., Fasullo, J., Jahn, A., Landrum, L., Stevenson, S., et al. (2016). Climate Variability and Change since 850 CE: An Ensemble Approach with the Community Earth System Model. *Bulletin of the American Meteorological Society, 97*(5), 735-754. http://journals.ametsoc.org/doi/abs/10.1175/BAMS-D-14-00233.1

Planton, Y. Y., Guilyardi, E., Wittenberg, A. T., Lee, J., Gleckler, P. J., Bayr, T., et al. (2021). Evaluating Climate Models with the CLIVAR 2020 ENSO Metrics Package. *Bulletin of the American Meteorological Society, 102*(2), E193-E217. https://journals.ametsoc.org/view/journals/bams/102/2/BAMS-D-19-0337.1.xml

Potts, K. (2021). Biomass Burning and Gas Flares create the extreme West African Aerosol Plume Which Perturbs the Hadley Circulation and thereby Changes Europe's Winter Climate. *Preprints.org*. https://doi.org/10.20944/preprints202108.0554.v3

Potts, K. (2022). How extreme apparitions of the volcanic and anthropogenic south east Asian aerosol plume trigger and sustain: El Niño and Indian Ocean Dipole events; and drought in south eastern Australia. First attribution and mechanism using Global Volcanism Program, Last Millennium Ensemble, MERRA-2 reanalysis and NASA satellite data. *Atmos. Chem. Phys. Discuss., 2022*, 1-45. https://acp.copernicus.org/preprints/acp-2022-362/

Privalsky, V. E., & Jensen, D. T. (1995). Assessment of the influence of ENSO on annual global air temperatures. *Dynamics of Atmospheres and Oceans, 22*(3), 161-178. https://www.sciencedirect.com/science/article/pii/037702659400400Q

Rayner, N. A., Parker, D. E., Horton, E. B., Folland, C. K., Alexander, L. V., Rowell, D. P., et al. (2003). Global analyses of sea surface temperature, sea ice, and night marine air temperature since the late nineteenth century. *Journal of Geophysical Research: Atmospheres, 108*(D14). https://agupubs.onlinelibrary.wiley.com/doi/abs/10.1029/2002JD002670

Ridley, J., Menary, M., Kuhlbrodt, T., Andrews, M., & Andrews, T. (2019). MOHC HadGEM3-GC31-MM model output prepared for CMIP6 CMIP historical. https://doi.org/10.22033/ESGF/CMIP6.6112

Schmidt, G. A., Bader, D., Donner, L. J., Elsaesser, G. S., Golaz, J. C., Hannay, C., et al. (2017). Practice and philosophy of climate model tuning across six US modeling centers. *Geosci. Model Dev., 10*(9), 3207-3223. https://gmd.copernicus.org/articles/10/3207/2017/

Seferian, R. (2018). CNRM-CERFACS CNRM-ESM2-1 model output prepared for CMIP6 CMIP. Retrieved from https://doi.org/10.22033/ESGF/CMIP6.1391

Seland, Ø., Bentsen, M., Olivié, D. J. L., Toniazzo, T., Gjermundsen, A., Graff, L. S., et al. (2019). NCC NorESM2-LM model output prepared for CMIP6 CMIP historical. Retrieved from https://doi.org/10.22033/ESGF/CMIP6.8036

Senior, C. A., Jones, C. G., Wood, R. A., Sellar, A., Belcher, S., Klein-Tank, A., et al. (2020). U.K. Community Earth System Modeling for CMIP6. *Journal of Advances in Modeling Earth Systems, 12*(9), e2019MS002004. https://agupubs.onlinelibrary.wiley.com/doi/abs/10.1029/2019MS002004

Shiogama, H., Abe, M., & Tatebe, H. (2019). MIROC MIROC6 model output prepared for CMIP6 ScenarioMIP. Retrieved from https://doi.org/10.22033/ESGF/CMIP6.898

Studies, N. G. I. f. S. (2019). NASA-GISS GISS-E2-2-G model output prepared for CMIP6 CMIP. Retrieved from https://doi.org/10.22033/ESGF/CMIP6.2081

Swart, N. C., Cole, J. N. S., Kharin, V. V., Lazare, M., Scinocca, J. F., Gillett, N. P., et al. (2019). CCCma CanESM5 model output prepared for CMIP6 CMIP historical-cmip5. Retrieved from https://doi.org/10.22033/ESGF/CMIP6.12553

Tsonis, A. A., Elsner, J. B., Hunt, A. G., & Jagger, T. H. (2005). Unfolding the relation between global temperature and ENSO. *Geophysical Research Letters, 32*(9). https://agupubs.onlinelibrary.wiley.com/doi/abs/10.1029/2005GL022875

UK-Met-Office. (2023). What are El Niño and La Niña? . Retrieved from https://www.metoffice.gov.uk/weather/learn-about/weather/oceans/el-nino

Venzke, E. (2013). *Volcanoes of the World. v. 4.9.1 (17 Sep 2020) http://dx.doi.org/10.5479/si.GVP.VOTW4-2013*.

Wang, C. (2018). A review of ENSO theories. *National Science Review, 5*(6), 813-825. https://doi.org/10.1093/nsr/nwy104

Ziehn, T., Chamberlain, M., Lenton, A., Law, R., Bodman, R., Dix, M., et al. (2019). CSIRO ACCESS-ESM1.5 model output prepared for CMIP6 CMIP. Retrieved from https://doi.org/10.22033/ESGF/CMIP6.2288

# Supporting Information

## Areas Used

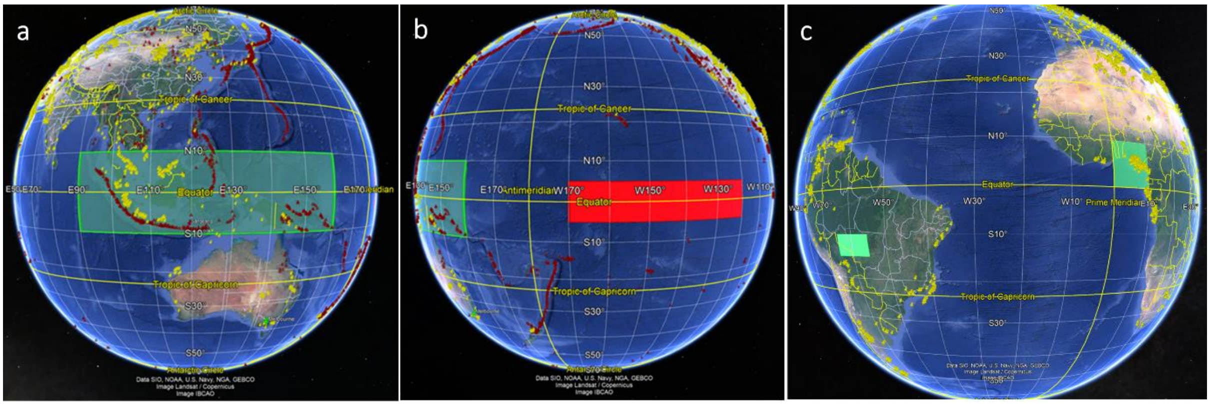


**Fig.S1 | a, SEAP Area. b, Nino 3.4 Area. c, SAMP and WAP Areas with volcanoes (red) and oil industry gas flares (yellow).**

| | HadISST1 | Canada | CSIRO | France | UK | Japan | NASA | NCAR | NOAA | Norway |
|---|---|---|---|---|---|---|---|---|---|---|
| 1870 | 0 | 0 | 0 | 0 | 1 | 0 | 0 | 0 | 0 | 0 |
| 1871 | 0 | 0 | 0 | 0 | 0 | 0 | 0 | 0 | 0 | 1 |
| 1872 | 0 | 0 | 0 | 0 | 0 | 0 | 1 | 1 | 0 | 0 |
| 1873 | 0 | 0 | 0 | 1 | 0 | 1 | 1 | 0 | 0 | 0 |
| 1874 | 0 | 0 | 0 | 0 | 0 | 0 | 0 | 0 | 0 | 0 |
| 1875 | 0 | 0 | 0 | 0 | 0 | 0 | 0 | 0 | 0 | 0 |
| 1876 | 0 | 0 | 0 | 0 | 0 | 0 | 0 | 0 | 0 | 0 |
| 1877 | 1 | 0 | 0 | 1 | 0 | 0 | 1 | 0 | 0 | 1 |
| 1878 | 1 | 0 | 0 | 0 | 0 | 0 | 1 | 0 | 0 | 1 |
| 1879 | 0 | 0 | 0 | 0 | 0 | 0 | 0 | 0 | 0 | 1 |
| 1880 | 0 | 0 | 0 | 0 | 0 | 0 | 0 | 1 | 0 | 1 |
| 1881 | 0 | 0 | 0 | 0 | 0 | 0 | 0 | 0 | 0 | 0 |
| 1882 | 0 | 0 | 0 | 1 | 0 | 1 | 0 | 0 | 0 | 0 |
| 1883 | 0 | 0 | 0 | 0 | 0 | 1 | 0 | 0 | 0 | 0 |
| 1884 | 0 | 0 | 0 | 0 | 0 | 0 | 0 | 0 | 0 | 0 |
| 1885 | 0 | 0 | 0 | 0 | 0 | 0 | 0 | 0 | 0 | 0 |
| 1886 | 0 | 0 | 0 | 0 | 0 | 0 | 0 | 0 | 0 | 0 |
| 1887 | 0 | 0 | 0 | 0 | 0 | 0 | 0 | 0 | 0 | 0 |
| 1888 | 1 | 1 | 0 | 0 | 0 | 1 | 0 | 0 | 1 | 0 |
| 1889 | 0 | 0 | 1 | 0 | 0 | 0 | 0 | 0 | 0 | 1 |
| 1890 | 0 | 0 | 0 | 1 | 0 | 0 | 0 | 0 | 0 | 0 |
| 1891 | 0 | 0 | 0 | 0 | 0 | 0 | 0 | 0 | 0 | 1 |
| 1892 | 0 | 0 | 0 | 0 | 0 | 0 | 0 | 0 | 0 | 0 |
| 1893 | 0 | 0 | 0 | 1 | 1 | 0 | 0 | 0 | 0 | 0 |
| 1894 | 0 | 0 | 0 | 1 | 0 | 0 | 1 | 0 | 0 | 1 |
| 1895 | 0 | 0 | 0 | 0 | 0 | 0 | 1 | 0 | 0 | 1 |
| 1896 | 1 | 0 | 0 | 0 | 1 | 0 | 0 | 0 | 0 | 0 |
| 1897 | 0 | 0 | 0 | 1 | 0 | 0 | 0 | 0 | 0 | 0 |

| | | | | | | | | | | |
|---|---|---|---|---|---|---|---|---|---|---|
| 1898 | 0 | 0 | 0 | 0 | 0 | 0 | 1 | 0 | 0 | 0 |
| 1899 | 0 | 0 | 0 | 0 | 0 | 1 | 0 | 0 | 1 | 0 |
| 1900 | 1 | 0 | 1 | 1 | 0 | 1 | 0 | 0 | 0 | 0 |
| 1901 | 0 | 0 | 0 | 0 | 0 | 1 | 0 | 0 | 0 | 0 |
| 1902 | 1 | 0 | 0 | 0 | 0 | 0 | 0 | 0 | 0 | 0 |
| 1903 | 0 | 0 | 0 | 1 | 0 | 0 | 0 | 1 | 0 | 1 |
| 1904 | 0 | 0 | 0 | 0 | 0 | 0 | 0 | 0 | 1 | 1 |
| 1905 | 1 | 0 | 0 | 0 | 0 | 0 | 1 | 0 | 0 | 0 |
| 1906 | 0 | 0 | 0 | 1 | 0 | 0 | 1 | 0 | 0 | 0 |
| 1907 | 0 | 0 | 0 | 0 | 0 | 0 | 0 | 0 | 0 | 0 |
| 1908 | 0 | 0 | 0 | 0 | 0 | 1 | 0 | 0 | 0 | 1 |
| 1909 | 0 | 0 | 0 | 0 | 0 | 1 | 0 | 0 | 0 | 1 |
| 1910 | 0 | 1 | 0 | 0 | 1 | 0 | 0 | 1 | 1 | 0 |
| 1911 | 0 | 1 | 1 | 1 | 0 | 0 | 0 | 0 | 0 | 0 |
| 1912 | 0 | 0 | 1 | 0 | 0 | 0 | 0 | 0 | 0 | 1 |
| 1913 | 0 | 0 | 0 | 0 | 1 | 0 | 1 | 0 | 0 | 0 |
| 1914 | 1 | 0 | 0 | 0 | 0 | 0 | 0 | 0 | 1 | 0 |
| 1915 | 0 | 0 | 1 | 0 | 0 | 0 | 0 | 0 | 0 | 0 |
| 1916 | 0 | 0 | 0 | 0 | 0 | 0 | 1 | 0 | 0 | 0 |
| 1917 | 0 | 0 | 0 | 0 | 0 | 1 | 0 | 0 | 0 | 0 |
| 1918 | 0 | 0 | 0 | 0 | 1 | 0 | 0 | 0 | 0 | 0 |
| 1919 | 1 | 0 | 0 | 1 | 1 | 0 | 1 | 0 | 1 | 1 |
| 1920 | 0 | 0 | 1 | 1 | 0 | 0 | 1 | 0 | 0 | 0 |
| 1921 | 0 | 0 | 0 | 0 | 0 | 0 | 0 | 0 | 0 | 0 |
| 1922 | 0 | 0 | 0 | 0 | 0 | 1 | 0 | 0 | 1 | 0 |
| 1923 | 0 | 0 | 1 | 0 | 1 | 1 | 1 | 0 | 1 | 1 |
| 1924 | 0 | 1 | 0 | 0 | 0 | 1 | 1 | 1 | 0 | 0 |
| 1925 | 0 | 0 | 1 | 0 | 0 | 0 | 1 | 0 | 0 | 0 |
| 1926 | 1 | 0 | 0 | 0 | 0 | 0 | 0 | 0 | 0 | 0 |
| 1927 | 0 | 0 | 0 | 1 | 1 | 0 | 0 | 0 | 1 | 1 |

| | | | | | | | | | | |
|---|---|---|---|---|---|---|---|---|---|---|
| 1928 | 0 | 1 | 0 | 0 | 1 | 0 | 0 | 1 | 0 | 0 |
| 1929 | 0 | 0 | 0 | 0 | 0 | 0 | 0 | 1 | 0 | 1 |
| 1930 | 1 | 0 | 0 | 0 | 0 | 0 | 0 | 0 | 0 | 0 |
| 1931 | 1 | 0 | 0 | 0 | 0 | 0 | 1 | 0 | 1 | 1 |
| 1932 | 0 | 0 | 0 | 0 | 0 | 0 | 0 | 0 | 1 | 0 |
| 1933 | 0 | 0 | 0 | 0 | 0 | 0 | 0 | 1 | 0 | 0 |
| 1934 | 0 | 0 | 1 | 0 | 0 | 0 | 1 | 1 | 0 | 0 |
| 1935 | 0 | 0 | 0 | 0 | 0 | 0 | 1 | 1 | 0 | 1 |
| 1936 | 0 | 0 | 0 | 0 | 0 | 1 | 0 | 1 | 0 | 0 |
| 1937 | 0 | 0 | 1 | 1 | 0 | 1 | 0 | 0 | 0 | 0 |
| 1938 | 0 | 0 | 0 | 0 | 0 | 0 | 1 | 0 | 0 | 0 |
| 1939 | 0 | 1 | 0 | 0 | 0 | 0 | 1 | 0 | 1 | 0 |
| 1940 | 1 | 1 | 0 | 0 | 1 | 0 | 0 | 0 | 0 | 1 |
| 1941 | 1 | 0 | 0 | 1 | 1 | 0 | 0 | 0 | 0 | 0 |
| 1942 | 0 | 0 | 1 | 0 | 0 | 0 | 0 | 1 | 0 | 0 |
| 1943 | 0 | 1 | 0 | 0 | 0 | 1 | 1 | 1 | 1 | 1 |
| 1944 | 0 | 0 | 0 | 0 | 1 | 1 | 0 | 0 | 0 | 0 |
| 1945 | 0 | 0 | 0 | 0 | 0 | 0 | 0 | 1 | 0 | 0 |
| 1946 | 0 | 1 | 0 | 0 | 0 | 0 | 0 | 0 | 0 | 0 |
| 1947 | 0 | 0 | 0 | 0 | 0 | 0 | 0 | 0 | 1 | 1 |
| 1948 | 0 | 1 | 0 | 0 | 0 | 1 | 0 | 0 | 0 | 0 |
| 1949 | 0 | 1 | 0 | 0 | 0 | 1 | 0 | 0 | 1 | 0 |
| 1950 | 0 | 0 | 0 | 0 | 0 | 0 | 0 | 0 | 0 | 1 |
| 1951 | 0 | 1 | 1 | 0 | 0 | 0 | 0 | 0 | 0 | 0 |
| 1952 | 0 | 0 | 0 | 0 | 1 | 0 | 0 | 1 | 1 | 0 |
| 1953 | 0 | 0 | 0 | 0 | 1 | 0 | 1 | 0 | 1 | 0 |
| 1954 | 0 | 0 | 1 | 1 | 0 | 0 | 1 | 0 | 0 | 1 |
| 1955 | 0 | 0 | 0 | 0 | 0 | 1 | 0 | 1 | 0 | 1 |
| 1956 | 0 | 0 | 0 | 0 | 0 | 1 | 0 | 1 | 0 | 0 |
| 1957 | 1 | 0 | 0 | 1 | 1 | 1 | 0 | 0 | 0 | 0 |

| | | | | | | | | | | |
|---|---|---|---|---|---|---|---|---|---|---|
| 1958 | 1 | 0 | 0 | 0 | 0 | 0 | 1 | 1 | 1 | 1 |
| 1959 | 0 | 0 | 0 | 0 | 0 | 0 | 1 | 1 | 1 | 1 |
| 1960 | 0 | 1 | 0 | 1 | 1 | 0 | 0 | 0 | 0 | 0 |
| 1961 | 0 | 0 | 1 | 0 | 0 | 0 | 0 | 1 | 0 | 0 |
| 1962 | 0 | 0 | 1 | 0 | 0 | 1 | 0 | 0 | 1 | 0 |
| 1963 | 0 | 0 | 0 | 0 | 0 | 0 | 1 | 0 | 0 | 0 |
| 1964 | 0 | 0 | 0 | 0 | 0 | 0 | 1 | 1 | 0 | 0 |
| 1965 | 1 | 1 | 0 | 0 | 0 | 0 | 0 | 0 | 0 | 1 |
| 1966 | 0 | 1 | 0 | 1 | 0 | 0 | 0 | 0 | 1 | 1 |
| 1967 | 0 | 0 | 0 | 0 | 0 | 1 | 0 | 1 | 1 | 0 |
| 1968 | 0 | 0 | 0 | 0 | 1 | 1 | 1 | 0 | 0 | 0 |
| 1969 | 1 | 0 | 0 | 0 | 0 | 0 | 1 | 0 | 0 | 0 |
| 1970 | 0 | 0 | 0 | 0 | 0 | 0 | 0 | 1 | 0 | 1 |
| 1971 | 0 | 0 | 0 | 0 | 0 | 0 | 0 | 1 | 0 | 0 |
| 1972 | 1 | 0 | 0 | 0 | 1 | 0 | 1 | 0 | 1 | 0 |
| 1973 | 0 | 1 | 1 | 1 | 0 | 0 | 1 | 0 | 0 | 0 |
| 1974 | 0 | 1 | 0 | 0 | 0 | 1 | 0 | 0 | 0 | 0 |
| 1975 | 0 | 0 | 0 | 0 | 0 | 1 | 0 | 0 | 0 | 0 |
| 1976 | 0 | 0 | 0 | 0 | 0 | 0 | 0 | 1 | 1 | 0 |
| 1977 | 1 | 1 | 0 | 1 | 1 | 0 | 0 | 0 | 1 | 0 |
| 1978 | 0 | 0 | 0 | 0 | 0 | 1 | 1 | 0 | 1 | 0 |
| 1979 | 0 | 0 | 0 | 0 | 0 | 0 | 1 | 1 | 0 | 0 |
| 1980 | 0 | 1 | 1 | 1 | 0 | 0 | 0 | 0 | 0 | 0 |
| 1981 | 0 | 1 | 0 | 0 | 0 | 0 | 0 | 0 | 1 | 1 |
| 1982 | 1 | 1 | 0 | 0 | 0 | 1 | 0 | 1 | 1 | 1 |
| 1983 | 1 | 0 | 1 | 0 | 0 | 1 | 0 | 1 | 0 | 1 |
| 1984 | 0 | 0 | 0 | 1 | 0 | 1 | 0 | 0 | 0 | 0 |
| 1985 | 0 | 0 | 0 | 1 | 0 | 0 | 1 | 0 | 0 | 0 |
| 1986 | 0 | 0 | 0 | 0 | 0 | 0 | 1 | 1 | 0 | 0 |
| 1987 | 1 | 0 | 0 | 0 | 0 | 0 | 0 | 1 | 0 | 0 |

| | | | | | | | | | | |
|---|---|---|---|---|---|---|---|---|---|---|
| 1988 | 0 | 0 | 0 | 0 | 0 | 0 | 0 | 0 | 0 | 0 |
| 1989 | 0 | 1 | 0 | 0 | 0 | 0 | 1 | 0 | 1 | 1 |
| 1990 | 0 | 0 | 0 | 0 | 1 | 0 | 1 | 1 | 1 | 1 |
| 1991 | 1 | 1 | 0 | 0 | 0 | 0 | 1 | 1 | 1 | 1 |
| 1992 | 1 | 0 | 0 | 1 | 1 | 1 | 0 | 0 | 0 | 0 |
| 1993 | 1 | 0 | 0 | 0 | 0 | 1 | 0 | 1 | 0 | 0 |
| 1994 | 0 | 0 | 0 | 0 | 0 | 1 | 0 | 0 | 0 | 0 |
| 1995 | 0 | 0 | 1 | 0 | 0 | 0 | 1 | 0 | 0 | 0 |
| 1996 | 0 | 1 | 0 | 0 | 1 | 0 | 0 | 0 | 0 | 0 |
| 1997 | 1 | 1 | 1 | 0 | 0 | 0 | 0 | 1 | 0 | 1 |
| 1998 | 0 | 1 | 1 | 0 | 0 | 1 | 0 | 0 | 0 | 0 |
| 1999 | 0 | 1 | 0 | 0 | 1 | 1 | 0 | 0 | 1 | 0 |
| 2000 | 0 | 1 | 0 | 1 | 0 | 0 | 1 | 1 | 1 | 1 |
| 2001 | 0 | 1 | 1 | 0 | 1 | 0 | 1 | 1 | 1 | 0 |
| 2002 | 1 | 1 | 1 | 0 | 0 | 0 | 0 | 1 | 0 | 0 |
| 2003 | 0 | 0 | 0 | 1 | 0 | 1 | 0 | 0 | 1 | 0 |
| 2004 | 0 | 1 | 1 | 1 | 0 | 1 | 0 | 0 | 1 | 1 |
| 2005 | 0 | 0 | 1 | 0 | 1 | 0 | 0 | 0 | 0 | 0 |
| 2006 | 0 | 0 | 0 | 0 | 1 | 0 | 0 | 1 | 0 | 0 |
| 2007 | 0 | 1 | 0 | 1 | 0 | 1 | 0 | 1 | 0 | 1 |
| 2008 | 0 | 0 | 1 | 1 | 0 | 1 | 1 | 0 | 1 | 1 |
| 2009 | 0 | 1 | 1 | 1 | 1 | 1 | 1 | 0 | 1 | 0 |
| 2010 | 0 | 1 | 1 | 1 | 1 | 0 | 0 | 0 | 0 | 1 |
| 2011 | 0 | 1 | 1 | 1 | 1 | 0 | 0 | 1 | 0 | 1 |
| 2012 | 0 | 0 | 1 | 0 | 0 | 1 | 0 | 1 | 1 | 0 |
| 2013 | 0 | 1 | 1 | 0 | 0 | 1 | 1 | 0 | 0 | 1 |
| 2014 | 0 | 1 | 1 | 0 | 1 | 0 | 1 | 0 | 0 | 1 |

**Table S1 | Years identified as ENSO years by the UK Met Office definition (Temperature more than 0.5C above the long term average.) from the HadlSST1 (highlighted in red) and the nine models analysed.**

| | HadlSST1 | Canada | CSIRO | France | UK | Japan | NASA | NCAR | NOAA | Norway | Average |
|---|---|---|---|---|---|---|---|---|---|---|---|
| **HadlSST1** | 1 | 0.034 | -0.092 | 0.018 | 0.086 | -0.050 | 0.004 | 0.003 | 0.058 | 0.079 | 0.016 |
| **Canada** | 0.034 | 1 | 0.223 | 0.124 | 0.158 | 0.070 | -0.025 | 0.054 | 0.216 | 0.145 | 0.111 |
| **CSIRO** | -0.092 | 0.223 | 1 | 0.176 | 0.006 | 0.055 | 0.066 | -0.002 | -0.060 | 0.066 | 0.049 |
| **France** | 0.018 | 0.124 | 0.176 | 1 | 0.148 | 0.068 | 0.042 | -0.203 | -0.005 | 0.077 | 0.050 |
| **UK** | 0.086 | 0.158 | 0.006 | 0.148 | 1 | -0.081 | 0.006 | -0.066 | 0.139 | -0.066 | 0.037 |
| **Japan** | -0.050 | 0.070 | 0.055 | 0.068 | -0.081 | 1 | -0.151 | -0.039 | 0.151 | -0.086 | -0.007 |
| **NASA** | 0.004 | -0.025 | 0.066 | 0.042 | 0.006 | -0.151 | 1 | 0.033 | 0.155 | 0.140 | 0.030 |
| **NCAR** | 0.003 | 0.054 | -0.002 | -0.203 | -0.066 | -0.039 | 0.033 | 1 | 0.068 | 0.131 | -0.002 |
| **NOAA** | 0.058 | 0.216 | -0.060 | -0.005 | 0.139 | 0.151 | 0.155 | 0.068 | 1 | 0.188 | 0.101 |
| **Norway** | 0.079 | 0.145 | 0.066 | 0.077 | -0.066 | -0.086 | 0.140 | 0.131 | 0.188 | 1 | 0.075 |
| **Average** | 0.016 | 0.111 | 0.049 | 0.050 | 0.037 | -0.007 | 0.030 | -0.002 | 0.101 | 0.075 | |

**Table S2 | Correlation matrix of Nino 3.4 temperature from the HadlSST1 dataset and the nine models.**

## The Eight Continental Scale Aerosol Plumes

The locations of the eight continental scale aerosol plumes are shown in Figures S1 and S2. The average monthly MERRA-2 AOD level[1] (1980 to 2020) of each plume is shown in Figure S3. Four plumes peak in the boreal summer, one in the boreal winter, two in September and one in August. The major sources of the plumes are shown in Table S1.

All plumes create local climate change when they exist, some cause regional change and at least one causes global change.

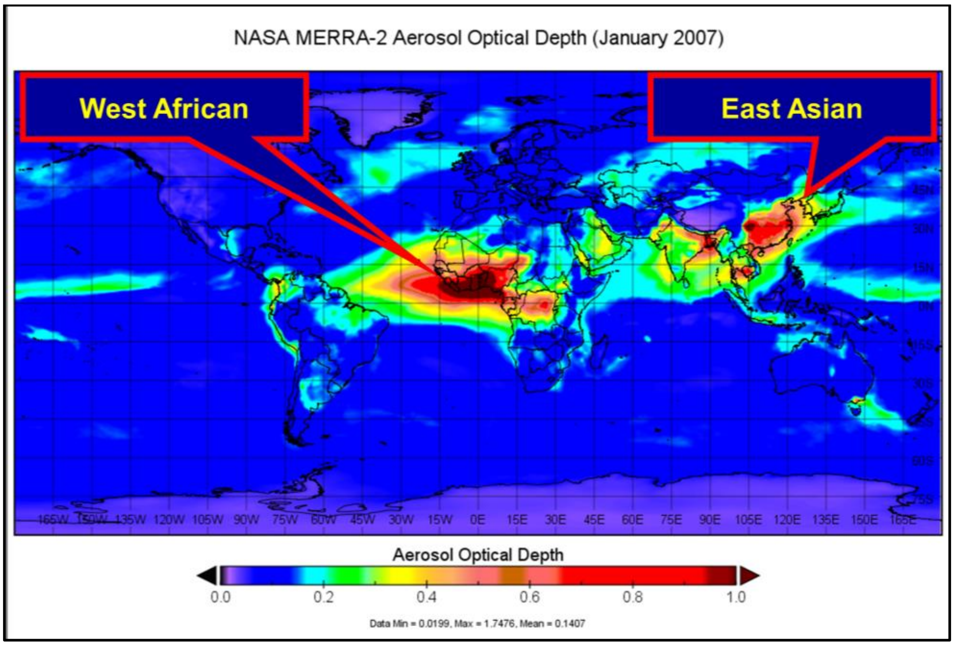


**Fig.S2 | MERRA-2 AOD Jan 2007 showing two of the eight plumes.**

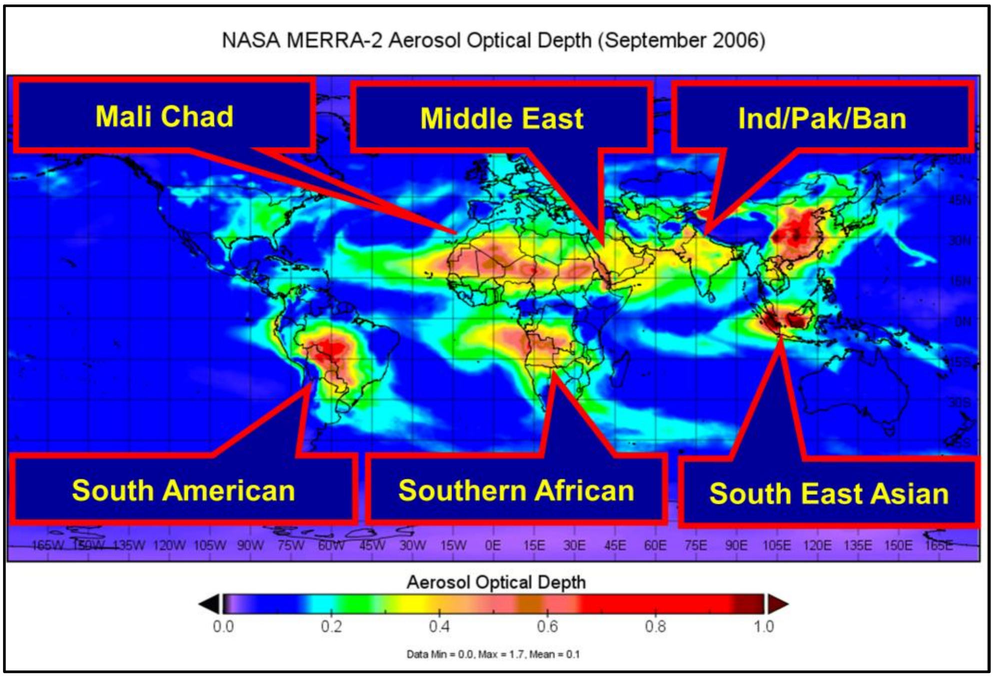


**Fig.S3 | MERRA-2 AOD September 2006 showing six of the eight plumes.**

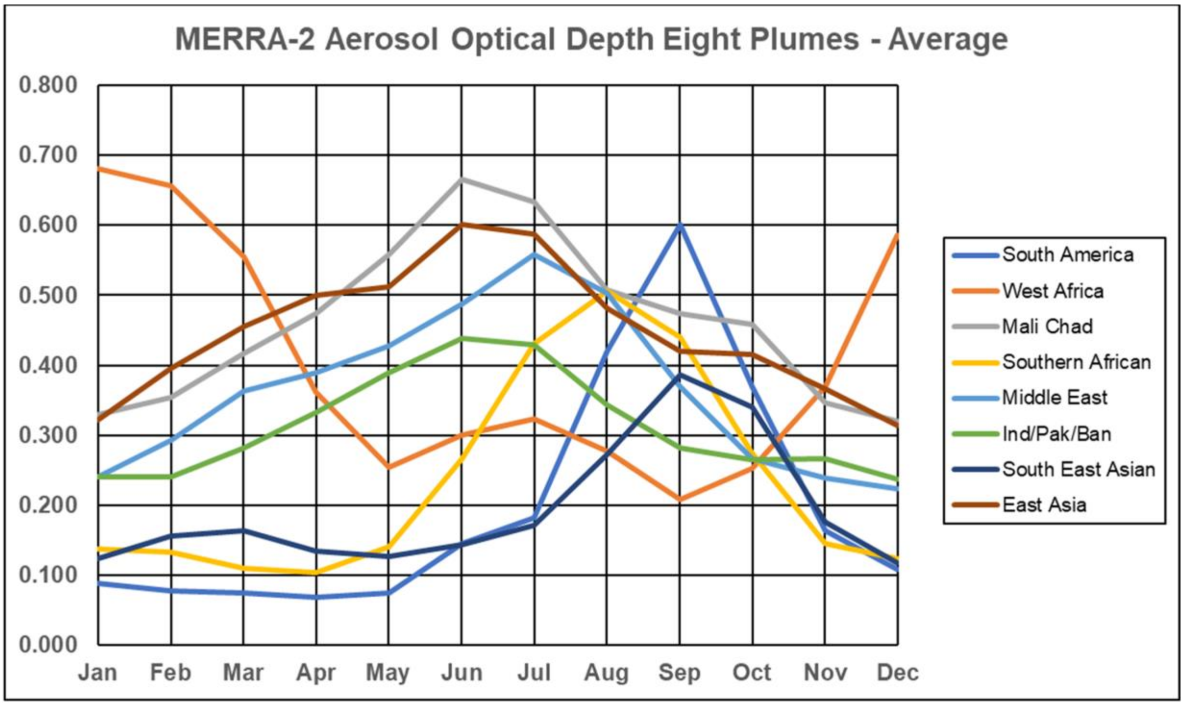


**Fig.S4 | Average monthly MERRA-2 AOD of the eight plumes 1980 to 2020.**

| Plume | Anthropogenic Source | Natural Source |
|---|---|---|
| South American | Biomass | Volcanoes |
| West African | Biomass, Gas Flares | Dust, Volcanoes |
| Mali/Chad | Peat fires under dried up lakes? | Dust |
| Middle East | Gas Flares | Dust, Volcanoes |
| Southern African | Biomass | Volcanoes, Dust |
| India/Pakistan/Bangladesh | Biomass, Industry | Dust |
| South East Asian | Biomass, Gas Flares | Volcanoes |
| East Asian | Industry, Biomass | Dust |

**Table S3 | The aerosol sources of the eight continental scale aerosol plumes.**